2
Flow and dispersion

In the simplest characterisation of solids, liquids, and gases, our perspective is influenced implicitly by both macroscopic and molecular standpoints, through our descriptors, fluidity and compressibility. Liquids and gases are fluids. They flow continuously when an external force is applied, whereas a solid will merely elastically deform until that external force is balanced by internal stress, returning to its original shape when the stress is removed. These mechanical ideas have their pedigree in Bernoulli, Hooke, and Newton. However, compressibility, significant in gases and vanishingly small in solids and liquids, is an idea rooted in the molecular and atomic model of matter, the former because in liquids and solids we picture molecules in close contact, and the latter because atomic incompressibility ultimately resides in the quantum mechanical principles associated with the Pauli exclusion principle.

Of course such a simplistic subdivision of matter is naive. Polymer networks, solid yet softly so, comprise considerable empty space. They are distinctly compressible. Gels, while dense and elastic, may start to flow once the applied stress exceeds a yield point. Many modern synthetic materials, most food products, and all biological tissues are neither simple solids nor liquids but comprise dispersed solid/liquid phases. Given sufficient time, that which appears solid on a human time scale may well appear fluid. In the song of Deborah [1], 'the mountains shall flow before the Lord'.

We will have occasion to reflect on material complexity in later chapters. Indeed, in the case of soft solids, complex fluids, or condensed matter comprising dispersed liquid/solid phases, nuclear magnetic resonance provides an almost ideal investigative tool, principal amongst the items in the NMR tool kit being the measurement of molecular translational motion. In Chapter 1 we traversed the diffusive motion that arises as a consequence of thermal fluctuations. Here we introduce ideas of flow driven by external stress, and of the stochastic fluctuations that arise when flow is directed through a porous solid matrix. In this latter case, known as dispersive flow, not only will the link with Brownian motion become clear, but we will see that dispersion offers an even richer spectrum of behaviours. We cannot, in one chapter, hope to cover all the essential ideas in fluid mechanics, and readers can find a more complete introduction in a number of texts dedicated to this subject [2–6]. We will, however, highlight a few key concepts, delving in greater depth into areas where NMR measurement of translational motion has the potential for useful insight.

Translational Dynamics and Magnetic Resonance, First Edition, Paul T. Callaghan, © Paul T. Callaghan 2011.
Published in 2011 by Oxford University Press.

2.1 Flow

2.1.1 Eulerian and Lagrangian descriptions

In describing fluid motion it is possible to adopt two standpoints [4]. In the first, known as the Eulerian perspective, fluid motion is described by assigning to each point in the space of a fluid, a time-dependent velocity $\mathbf{v}_E(\mathbf{r}, t)$. The set of velocities at different spatial locations represent a velocity field. In the special case where that field is constant with time (steady-state flow), the Eulerian velocity field may be simply written $\mathbf{v}_E(\mathbf{r})$. Note that in magnetic resonance imaging experiments we are, in principle, able to 'map the velocity field'—in other words to measure at each location $\mathbf{r}$, $\mathbf{v}_E(\mathbf{r})$ in the case of steady-state flow, indexflow!steady state or $\mathbf{v}_E(\mathbf{r}, t)$ in the case of fluctuating flow, limited as always by some predetermined spatial and temporal resolution.

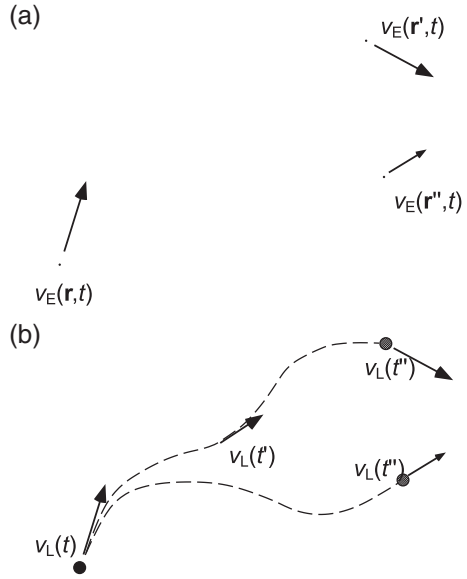

Fig. 2.1 (a) The Eulerian velocity field at time t and three separate locations $\mathbf{r}$, $\mathbf{r}'$, and $\mathbf{r}''$. (b) The Lagrangian velocity trajectories over time t for two particles in the ensemble starting in close proximity at $\mathbf{r}$, each of which has finite probability of passing, at time t'', through positions $\mathbf{r}'$, and $\mathbf{r}''$. Their velocities at time t'' will be identical to $v_E(\mathbf{r}')$ and $v_E(\mathbf{r}'')$, respectively, if the Eulerian velocity field is steady state.

The second standpoint is known as the Lagrangian perspective and it describes motion in terms of the history of individual fluid particles. For each particle, a time-dependent position $\mathbf{r}_L(t)$ or velocity $\mathbf{v}_L(t)$ is assigned and, for the fluid as a whole, these vectors represent one member of an ensemble of particle positions or velocity vectors. The members of that ensemble could be labelled in different ways, but one example might be to assign to each particle its position, $\mathbf{r}_0$ when $t = 0$. Hence we could speak of the history of positions or motion of the particle starting at $\mathbf{r}_0$ as $\mathbf{r}_L(\mathbf{r}_0, t)$

or $\mathbf{v}_L(\mathbf{r}_0, t)$. Equally we could label each particle, through a component atom, by its nuclear spin magnetisation at some suitable time origin. It is precisely that approach which we may use in magnetic resonance where, even if no imaging gradients are applied, the evolution of individual spin magnetisation may be tracked, albeit as a contribution to some ensemble average taken over the entire fluid sample. For such averaging methods, the Lagrangian perspective is natural. Generally, we will omit the label (for example $\mathbf{r}_0$) and simply note that we must deal with an ensemble of histories $\{\mathbf{r}_L(t)\}$ and $\{\mathbf{v}_L(t)\}$.

Figure 2.1 shows the relationship between the Eulerian and Lagrangian perspectives in the case where the Eulerian field happens to be steady state, and for a particular case where particles beginning in the same vicinity have a finite probability of passing through two different positions in the Eulerian velocity field at a later time t''. In this case there is a simple probabilistic assignment of $v_L(t)$ to $v_E(\mathbf{r})$, a matter which we will analyse in detail later.

The type of flow depicted in Fig. 2.1 is dispersive. Figure 2.2 depicts flow fields in which the flow is, respectively, laminar, turbulent, and dispersive. In laminar flow,

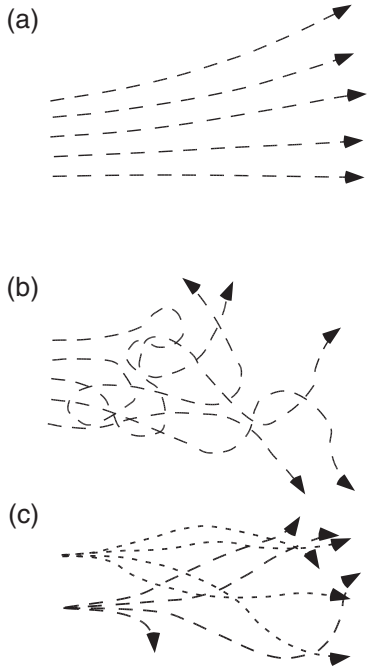

Fig. 2.2 (a) Steady state laminar flow in which no streamlines cross. (b) Turbulent flow in which the local Eulerian velocities fluctuate with time. (c) Dispersive flow. Particles starting together on the same streamline subsequently follow divergent paths. Dispersive flow can arise from turbulence but may also be associated with laminar flow in a complex porous matrix. The different dashed paths represent subsequent flow histories from different starting points. In steady state flow there are no streamline crossings but trajectories can cross above and below one another in three dimensional flow.

particles starting in nearby proximity follow a time course in which the fluid between them is confined within laminae bounded by the particle streamlines. The laminar flow field is inherently steady state. By contrast, in turbulence the flow field fluctuates in an irregular manner, most commonly due to the effect of fluid inertia at high flow rates where non-linearities start to influence the equations of motion. And, in dispersive flow, while the flow may be steady state, particles that occupy a nearby location at a particular time may subsequently follow very different and diverging paths. Such dispersive flow is characteristic of fluid moving through a porous medium. The non-laminar examples illustrate why the use of a starting coordinate may be a poor descriptor for the Lagrangian ensemble, irrespective of whether the flow field fluctuates or is in steady state.

For two particles that occupy an infinitesimally close location at a particular time, we may, in steady state, use the conditional probability introduced in Chapter 1 to describe the likelihood of different subsequent paths. $P(\mathbf{r}|\mathbf{r}', t)$ describes the probability that a particle with Eulerian velocity $\mathbf{v}_E(\mathbf{r})$ at time zero will have Eulerian velocity $\mathbf{v}_E(\mathbf{r}')$ at time t. That conditional probability will have the form of a Dirac delta function for laminar flow. In other words, we may, in the case of laminar flow, predict with certainty where a fluid particle passing through a particular location will end up at any later time. By contrast, for turbulent or dispersive flow the conditional probability will have more complex structure. As we shall see later in section 8.4, $P(\mathbf{r}|\mathbf{r}', t)$ will provide a valuable tool in linking the Eulerian and Lagrangian descriptions of flow field dynamics.

2.1.2 Substantive derivative and fluid dynamics

In the following sections we will write down some equations of motion for fluid mechanics [7, 8]; equations which have their origin in Newtonian dynamics. That origin raises an interesting issue when we come to describe fluid particle acceleration, since any time derivative of velocity, $\partial \mathbf{v}_E(\mathbf{r},t)/\partial t$, taken in the Eulerian perspective, will not tell us about the acceleration of a particular particle, but instead represents the rate at which the velocity at a particular point is changing as different particles pass through. The derivative we seek, $\partial \mathbf{v}_L(t)/\partial t$, belongs to a single particle and must be calculated in a co-moving frame. Let us consider such a co-moving frame derivative for any quantity $A(\mathbf{r}, t)$, given that the local Eulerian velocity is $\mathbf{v}_E(\mathbf{r}, t)$. We will drop the E subscript in what follows and allow that $\mathbf{v}(\mathbf{r}, t)$ is implicitly Eulerian. At a time later by dt, the fluid particles starting at $\mathbf{r}$ have moved to $\mathbf{r} + dt\,\mathbf{v}$, displacement dx being simply $dt\,v_x$, where v_x is the x component of the velocity, and so on. Hence the change in A to first order may be written [4] via a Taylor expansion as

$$\begin{aligned} dA &= dt\frac{\partial A}{\partial t} + dx\frac{\partial A}{\partial x} + dy\frac{\partial A}{\partial y} + dz\frac{\partial A}{\partial z} \\ &= dt\frac{\partial A}{\partial t} + dt\,v_x\frac{\partial A}{\partial x} + dt\,v_y\frac{\partial A}{\partial y} + dt\,v_z\frac{\partial A}{\partial z} \\ &= dt\frac{\partial A}{\partial t} + dt\,\mathbf{v}\cdot\nabla A \end{aligned} \tag{2.1}$$

For the frame moving with the fluid, the points $\mathbf{r}$ and $\mathbf{r} + \mathbf{v}\,dt$ are of course coincident and so dA/dt is the same as $\partial A/\partial t$ in the co-moving frame. In the stationary frame, dA/dt is called the 'substantive derivative', $\mathcal{D}A/\mathcal{D}t$, and written

$$\frac{\mathcal{D}A}{\mathcal{D}t} = \frac{\partial A}{\partial t} + (\mathbf{v} \cdot \nabla)\, A \tag{2.2}$$

The term $(\mathbf{v} \cdot \nabla)$ is sometimes called the advective or convective component of the substantive derivative $\mathcal{D}/\mathcal{D}t$.

A first example of the use of this substantive derivative concerns the continuity equation, which states that the divergence of mass flow is related to the local change in density by

$$\rho \nabla \cdot \mathbf{v} = -\frac{\mathcal{D}\rho}{\mathcal{D}t} \tag{2.3}$$

The second is the so-called 'momentum equation', which relates the acceleration of the particles to the net force applied

$$-\nabla p + \mathbf{f} = \rho \frac{\mathcal{D}\mathbf{v}}{\mathcal{D}t} \tag{2.4}$$

In this version of Newton's second law, the forces (expressed per unit volume) arise from the pressure gradient and from body forces ($\mathbf{f}$) acting on the fluid, an example of the latter being the gravitational force per unit volume ($\rho\mathbf{g}$). Note again, the velocity $\mathbf{v} = \mathbf{v}(\mathbf{r}, t)$ is implicitly Eulerian, and will be so for the rest of this book, unless stated otherwise.

Equations 2.3 and 2.4 are together known as Euler's equations, corresponding respectively to laws of mass and momentum conservation.[1] They apply for the case of inviscid flow, that is when there is no dissipation of energy due to fluid viscosity.

2.1.3 Navier–Stokes, inertia, and the Reynolds number

When viscosity plays a role, the Euler equation must be expanded to read[2]

$$-\nabla \cdot \left(p \underline{\underline{\mathbf{I}}}\right) + \nabla \cdot \underline{\underline{\sigma}} + \mathbf{f} = \rho \frac{\mathcal{D}\mathbf{v}}{\mathcal{D}t} \tag{2.5}$$

where the identity matrix, also known as the unit tensor, is

$$\underline{\underline{\mathbf{I}}} = \begin{pmatrix} 1 & 0 & 0 \\ 0 & 1 & 0 \\ 0 & 0 & 1 \end{pmatrix} \tag{2.6}$$

and $\underline{\underline{\sigma}}$ is the deviatoric part of the stress tensor, explained in detail in the next section. Meanwhile, it is sufficient to note that for a liquid with constant dynamic viscosity, η, eqn 2.5 may be written

$$-\nabla p + \eta \nabla^2 \mathbf{v} + \mathbf{f} = \rho \frac{\mathcal{D}\mathbf{v}}{\mathcal{D}t} \tag{2.7}$$

Equation 2.7 is known as the Navier–Stokes equation [7, 8]. For an incompressible fluid we have the additional relation $\nabla \cdot \mathbf{v} = 0$.

[1] There is a third Euler equation for energy conservation, which need not concern us here.

[2] Note that we are treating the density, ρ, as constant, as would be appropriate for incompressible fluids, for example liquids.

Note that the convective part of the substantive derivative of velocity, $\rho(\mathbf{v}\cdot\nabla)\mathbf{v}$, is non-linear in the velocity and, when dominant, may lead to turbulent solutions of the Navier–Stokes equation. By contrast, the remaining terms are linear and, in the absence of convective effects, lead to well-defined solutions. The relative size of the convective and viscous terms may be described by a dimensionless number, obtained by non-dimensionalising eqn 2.7 using a characteristic length L and velocity v so that $\eta\nabla^2\mathbf{v}$ is of order $\eta v/L^2$ while $\rho(\mathbf{v}\cdot\nabla)\mathbf{v}$ is of order $\rho v^2/L$. This dimensionless number is known as the Reynolds number [9] and is defined by

$$\mathcal{R}_e = \frac{\rho v^2/L}{\eta v/L^2} = \frac{\rho v L}{\eta} = \frac{vL}{\nu} \tag{2.8}$$

where ν is the kinematic viscosity, η/ρ. For low Reynolds numbers the flow in simple geometries will be laminar, with a transition to turbulent flow for $\mathcal{R}_e \gg 1000$.

2.1.4 Stress and strain tensors

The dissipation of energy due to viscous drag, referred to in the previous section, is a consequence of deformational (shape-changing) flow. In simple terms, fluid deformation dissipates energy, while in the case of a solid, deformation causes energy to be stored elastically. In contrast, biological tissue, most foods, and a wide range of modern polymeric materials of interest all have both solid- and liquid-like properties and are consequently termed viscoelastic. Such complex fluids or soft solids are discussed in detail in Section 2.2.

The cause of deformation in materials is applied stress, quite simply the force applied per unit surface area, and the tensorial property of stress arises because of the independent directions associated with the force and the surface normal. The consequential deformation is also a tensor, the indices labelling both the direction of elemental displacements and the direction with respect to which those displacements vary.

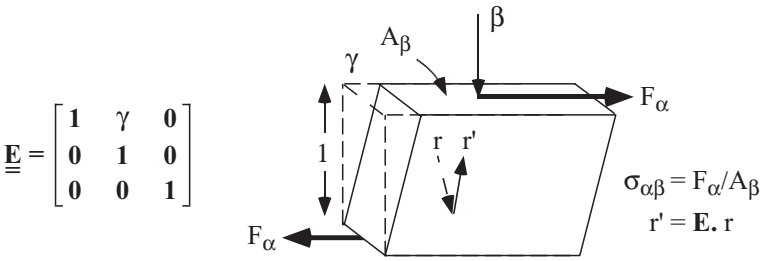

Fig. 2.3 Element of material subject to applied stress. Components of stress tensor $\sigma_{\alpha\beta}$ and deformation gradient tensor $E_{\alpha\beta}$ are shown.

Figure 2.3 shows an element of material subject to an applied stress. We choose to describe an element of the stress tensor $\underline{\underline{\sigma}}$ by $\sigma_{\alpha\beta}$, where the indices indicate the direction of the force and the relevant surface normal. A corresponding deformation in which a point defined by vector $\mathbf{r}$ is displaced to the position $\mathbf{r}'$ may be defined by the dimensionless strain or deformation gradient tensor

$$E_{\alpha\beta} = \frac{\partial r'_\alpha}{\partial r_\beta} \tag{2.9}$$

where $\mathbf{r}' = \underline{\underline{\mathbf{E}}} \cdot \mathbf{r}$ and α,β may be taken to represent components of the Cartesian axis frame. A shear deformation is given by

$$\underline{\underline{\mathbf{E}}} = \begin{pmatrix} 1 & \gamma & 0 \\ 0 & 1 & 0 \\ 0 & 0 & 1 \end{pmatrix} \tag{2.10}$$

while a volume-conserving uniaxial elongation (along the z-axis) is given by

$$\underline{\underline{\mathbf{E}}} = \begin{pmatrix} \lambda^{-1/2} & 0 & 0 \\ 0 & \lambda^{-1/2} & 0 \\ 0 & 0 & \lambda \end{pmatrix} \tag{2.11}$$

In elastic solids, a shear stress results in a fixed strain and for small strains ($\gamma \ll 1$) the relevant elastic modulus, G, is given by Hooke's law

$$\sigma_{xy} = G\gamma \tag{2.12}$$

In a liquid the deformation under applied stress is continuous and the material flows. Furthermore, the absence of unbalanced torques in a liquid leads to the requirement that the stress tensor be symmetric. Suppose we describe the flow in the liquid by the spatially dependent Eulerian velocity, $\mathbf{v}(\mathbf{r})$. Then the rate of strain tensor $\underline{\underline{\kappa}} = \nabla\mathbf{v}$ is defined by

$$\kappa_{\alpha\beta} = \frac{\partial v_\alpha}{\partial r_\beta} \tag{2.13}$$

For a Newtonian fluid the total stress tensor may be written in terms of the rate of strain tensor via the simple constitutive equation

$$\begin{aligned} T_{\alpha\beta} &= \eta\left(\kappa_{\alpha\beta} + \kappa_{\beta\alpha}\right) - pI_{\alpha\beta} \\ &= \sigma_{\alpha\beta} - pI_{\alpha\beta} \end{aligned} \tag{2.14}$$

where η is the constant viscosity, p is the isotropic pressure and $\sigma_{\alpha\beta}$ is the deviatoric part of the stress tensor. Note the sign convention used. External forces bearing on the fluid element and acting normal to the surface are positive when directed inward. By contrast, the intrinsic pressure arising from the fluid element acts outward at the surface normal. In discussing the viscous behaviour of liquids it is customary to neglect the isotropic pressure term in eqn 2.14. However, it is important to note that the force driving the momentum change in the Navier–Stokes equation is related to the gradient in the total stress. Equations 2.5 and 2.7 retain the gradient in both the deviatoric part of the stress, $\underline{\underline{\sigma}}$, as well as in the isotropic pressure term.

$(\kappa_{\alpha\beta} + \kappa_{\beta\alpha})$ is the symmetric rate of strain tensor, sometimes denoted $2\underline{\underline{\mathbf{D}}} = \nabla\mathbf{v} + \nabla\mathbf{v}^T$. An antisymmetric (vorticity) part of the velocity gradient may be defined by $2\underline{\underline{\omega}} = \nabla\mathbf{v} - \nabla\mathbf{v}^T$. One may then conveniently represent eqn 2.14 as

$$\underline{\underline{\sigma}} = 2\eta\underline{\underline{\mathbf{D}}} \tag{2.15}$$

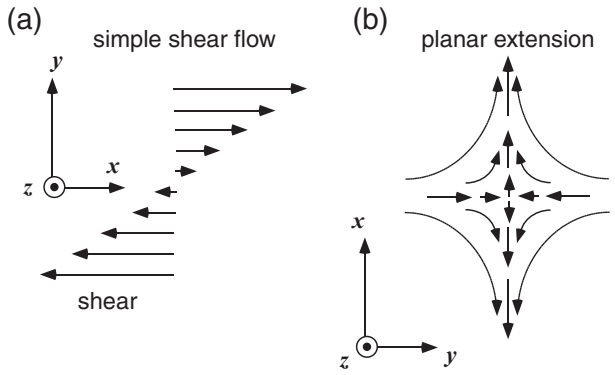

Fig. 2.4 Examples of velocity fields that result in (a) simple shear (across the flow) and (b) planar extension (at the central stagnation point).

As a simple example consider the simple shear case illustrated in Fig. 2.4. The velocity is everywhere directed along x and varies along y. Hence the only non-zero value of $\nabla\mathbf{v}$ is $\dot{\gamma} = {}^{\partial v_x}/_{\partial y}$. In this case

$$\nabla\mathbf{v} = \begin{pmatrix} 0 & \dot{\gamma} & 0 \\ 0 & 0 & 0 \\ 0 & 0 & 0 \end{pmatrix} \tag{2.16}$$

and

$$\underline{\underline{\mathbf{D}}} = \frac{1}{2}\begin{pmatrix} 0 & \dot{\gamma} & 0 \\ \dot{\gamma} & 0 & 0 \\ 0 & 0 & 0 \end{pmatrix} \tag{2.17}$$

and

$$\underline{\underline{\sigma}} = \eta\begin{pmatrix} 0 & \dot{\gamma} & 0 \\ \dot{\gamma} & 0 & 0 \\ 0 & 0 & 0 \end{pmatrix} \tag{2.18}$$

Clearly this result gives us the Newtonian viscosity law for fluids corresponding to Hooke's law for solids (eqn 2.12),

$$\sigma_{xy} = \eta\dot{\gamma} \tag{2.19}$$

Also shown in Fig. 2.4 is the case of planar extensional flow. This flow field contains sheared elements but at the centre is a stagnation point at which purely extensional flow results, and where

$$\underline{\underline{\mathbf{D}}} = \begin{pmatrix} \dot{\epsilon} & 0 & 0 \\ 0 & -\dot{\epsilon} & 0 \\ 0 & 0 & 0 \end{pmatrix} \tag{2.20}$$

2.1.5 Navier–Stokes solutions and lattice Boltzmann

Exact solutions to the Navier–Stokes equation for a Newtonian fluid are possible when the Reynolds number is small. One simple example concerns flow in a long cylindrical pipe of radius a. The steady-state pipe flow is laminar and directed along the axis

(z) of the pipe, with non-slip boundary conditions ($v_z = 0$) at the wall ($r = a$).[3] The natural coordinates are cylindrical polar (r, θ, z) and, by symmetry, the velocity is directed along z such that $v_r = v_\theta = 0$ and v_z is a function of r only. The substantive derivative is exactly zero in this problem, but the solution may be unstable to small symmetry-breaking perturbations if $\mathcal{R}_e$ is large. However, we will examine the low Reynolds number case and hence we may write eqn 2.7, in the absence of body forces, as

$$-\nabla p + \eta \nabla^2 \mathbf{v} = 0 \tag{2.21}$$

or, in cylindrical polars, and consistent with the symmetry outlined above

$$-\frac{\partial p}{\partial z} + \eta \frac{1}{r} \frac{\partial}{\partial r} \left(r \frac{\partial v_z(r)}{\partial r} \right) = 0 \tag{2.22}$$

The solution is clearly

$$v_z(r) = v_0 \left(1 - \frac{r^2}{a^2} \right) \tag{2.23}$$

where

$$v_0 = \frac{a^2}{4\eta} \frac{\partial p}{\partial z} \tag{2.24}$$

This velocity distribution is known as Poiseuille flow [10].[4] Note that v_0 is the

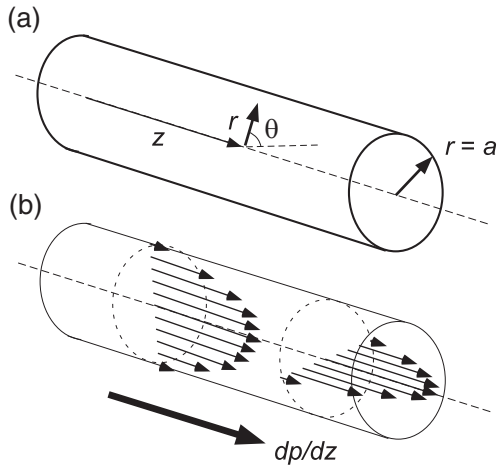

Fig. 2.5 (a) Pipe showing cylindrical polar coordinates and (b) Poiseuille flow profile.

maximum velocity at the pipe centre. It is easy to show that the mean velocity, averaged across the pipe, is $v_0/2$, and that the flow rate $\dot{Q} = \int_0^a 2\pi\, r\, v_z(r)\, dr$ is

[3]We shall assume here that the flow to be described is a long way from the entrance to the pipe, and that the pipe diameter is larger than the nanometre scale, where slip effects are apparent even in simple liquids.

[4]This pipe flow velocity profile was discovered independently by G. H. L. Hagen, who did his experiments at the same time as Poiseuille and before the year of Poiseuille's publication. In consequence it is often called the Hagen–Poiseuille law.

$$\dot{Q} = \frac{\pi a^4}{8\eta}\frac{\partial p}{\partial z} \tag{2.25}$$

Hence, for a known pressure gradient ($\partial p/\partial z$) down a pipe of radius a, the flow rate provides a simple indication of the viscosity.

The ability to ignore the non-linear effects of convection in the substantive derivative of the Navier–Stokes equation is possible only at low $\mathcal{R}_e$ or for certain regular geometries where symmetry requires $(\mathbf{v}\cdot\nabla)\,\mathbf{v} = 0$. General solutions are a challenge, even for numerical methods, and in complex flows such as the movement of liquids through a packed bed or porous matrix, conventional finite difference or finite element numerical solutions to the Navier–Stokes equation are prohibitively expensive in computer time, even when inertial effects may be neglected. However, an entirely different approach, known as the lattice Boltzmann method [11], provides a particularly efficient route to numerical solution.

Lattice Boltzmann (L-B) relies on the use of a finite lattice of points between which a gas of particles is convected at each time step of a simulation, and at which intersecting particles collide and separate according to rules that can inherently match the requirements of the Navier–Stokes equation. In the case of an incompressible fluid, there is also a requirement that the flow be divergence-less. In a sense, it mirrors a cellular automata approach to physical modelling, but with one important difference. The use of discrete particles in lattice gas automata methods introduces statistical noise as a consequence of the finite number of particles and lattice points. L-B avoids this problem by pre-averaging the lattice gas, replacing the Boolean particle number at each lattice node with an ensemble-averaged density distribution function. In this, the method follows the famous Boltzmann theory for atomistic dynamics.

Boltzmann introduced a probability density $f(\mathbf{r}, \mathbf{p}, t)$ in the 'phase space' of particle positions and momenta. The dynamical equation for this one-body distribution function may be written

$$\left(\frac{\partial}{\partial t} + \frac{\mathbf{p}}{m}\cdot\nabla + \mathbf{F}\cdot\nabla_{\mathbf{p}}\right) f(\mathbf{r}, \mathbf{p}, t) = C_{12} \tag{2.26}$$

where the right-hand side represents the interparticle two-body collisions and accounts for gain and loss components as particles stream in or out of the collision point. $\mathbf{F}$ is the external force, equivalent by Newtonian mechanics to $d\mathbf{p}/dt$, while $\nabla_{\mathbf{p}}$ is the vector derivative with respect to the components of momentum. Note the formal similarity of the left-hand side of eqn 2.26 to the substantive derivative of eqn 2.2, the additional momentum derivative term reflecting the influence of the force field. In Boltzmann's treatment the collision term involves two-body distribution functions that are reduced to a simple product of uncorrelated single-body distributions, with local equilibrium defined by a balance of particle gain and loss at each point. Out of that equilibrium comes the famous Maxwell–Boltzmann distribution of eqn 1.25.

The L-B method discretises the Boltzmann equation by dividing space into a set of lattice points (i) and limiting the velocities to a discrete set $\mathbf{v}_i$. The lattice Boltzmann equation is therefore

$$f_i(\mathbf{r}_i + \Delta\mathbf{r}, t + \Delta t) - f_i(\mathbf{r}_i, t) = C_i \tag{2.27}$$

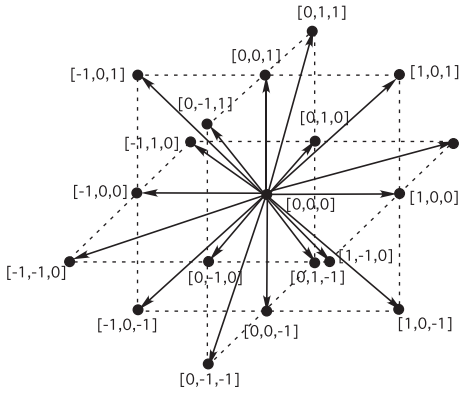

Fig. 2.6 D3Q19 lattice showing the 19 microscopic velocity directions, $\mathbf{v}_i$.

In implementing the lattice Boltzmann equation method for the case of Navier–Stokes flow of a viscous fluid, the collision operator, C_i, takes a form which allows for a single exponential relaxation towards the equilibrium distribution, the relaxation time reflecting the kinematic viscosity of the simulated fluid. One of the most famous forms of the collision operator is that due to Bhatnagar, Gross, and Krook [12], the so-called BGK operator. Note that a number of different lattice geometries are possible, for example the 3-D nineteen velocity (D3Q19) lattice shown in Fig. 2.6. For each lattice node $\mathbf{r}_i$ at time t there are 19 lattice directions labelled by i around the node, as shown in the figure. The local density and velocity of the fluid is then given by $\rho = \sum_i f_i$ and $\mathbf{v} = \rho^{-1} \sum_i f_i \mathbf{v}_i$. A particular advantage of L-B methods is that different boundary conditions are easily accommodated and the code is particularly amenable to parallelisation. A complete description of L-B methods would require a book on its own and readers can find further details in references [11, 13, 14].

2.1.6 Conditional probability and average propagators for flow

The conditional probability for steady-state laminar flow is exceptionally simple. We have certain knowledge as to the subsequent destination $\mathbf{r}'$ of a particle starting at any point $\mathbf{r}$ in the Eulerian flow field, and so we may use a Dirac delta function to describe $P(\mathbf{r}|\mathbf{r}', t)$. While the Navier–Stokes equation ignores Brownian motion, we need to bear in mind that these stochastic molecular excursions will always be superposed on that continuum flow. Generally this may be done by adding the Brownian motion in the co-moving frame.

Let us take a simple example in which all particles in a fluid have common velocity, $\mathbf{V}$. The conditional probability, allowing for flow alone will be

$$P(\mathbf{r}|\mathbf{r}', t) = \delta(\mathbf{r}' - (\mathbf{r} + \mathbf{V}t)) \tag{2.28}$$

The effect of adding the Brownian motion in the co-moving frame is simply to convolve the Brownian and flow probabilities via

$$\begin{aligned} P(\mathbf{r}|\mathbf{r}', t) &= \delta(\mathbf{r}' - (\mathbf{r} + \mathbf{V}t)) \otimes (4\pi Dt)^{-\frac{3}{2}} \exp\left(-\frac{(\mathbf{r}' - \mathbf{r})^2}{4Dt}\right) \\ &= (4\pi Dt)^{-3/2} \exp\left(-\frac{(\mathbf{r}' - (\mathbf{r} + \mathbf{V}t))^2}{4Dt}\right) \end{aligned} \tag{2.29}$$

The convolution $\otimes$ is defined by the *faltung* or folding integral

$$f(t) \otimes g(t) = \int_{-\infty}^{\infty} f(t')\, g(t - t')\, dt' \tag{2.30}$$

Note that the conditional probability of eqn 2.29 is, in this special case, independent of the starting position $\mathbf{r}$ and depends only on the displacement $\mathbf{R} = \mathbf{r}' - \mathbf{r}$. Hence, averaging over all starting positions we obtain the average propagator with identical form

$$\bar{P}(\mathbf{R}, t) = (4\pi Dt)^{-\frac{3}{2}} \exp\left(-\frac{(\mathbf{R} - \mathbf{V}t)^2}{4Dt}\right) \tag{2.31}$$

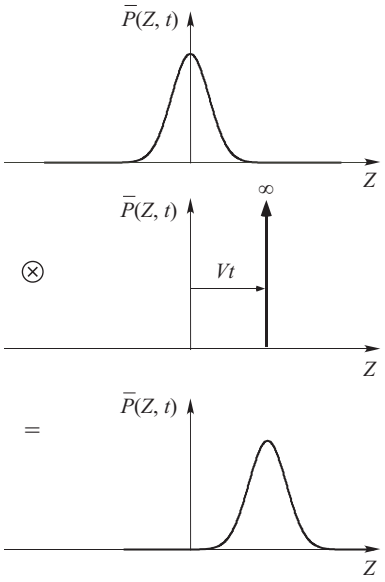

Fig. 2.7 Convolution of propagators for diffusion (top) and flow (middle) to obtain average propagator of eqn 2.31 (bottom). Note that this is a 1-D depiction in which the displacement $\mathbf{R}$ is replaced by Z.

Of course, when the flow field is not uniform, as in the case of pipe flow, for which the velocity varies as a function of radius, the description of the conditional probability is much more complicated when diffusion is included. Here Brownian migration

transverse to the flow direction results in particles changing streamlines, moving in effect to positions where the flow velocity differs. Hence, a small change in transverse position due to diffusion may lead to a subsequently wide separation in longitudinal position as the different velocities in adjacent streamlines have the effect of sweeping apart particles that had initially started together. This subtle and complex interplay of diffusion and flow heterogeneity is known as 'Taylor dispersion' [15], and, in the case of pipe flow, is discussed in some detail in Section 2.3.4. In the case of the more complex fluid flow in porous media, Taylor dispersion is one of several mechanisms that cause initially adjacent particles to become separated. These dispersion effects are of immense practical significance and are a major topic of this book. The facility of NMR to provide useful insight regarding dispersion is one of the reasons why NMR of porous media is a major area of international research.

While, for uniform flow, the average propagator, $\bar{P}(\mathbf{R}, t)$, is identical to the conditional probability, in the case of heterogeneous flow, it will differ. As an illustration we calculate the average propagator for pipe flow, choosing for simplicity a pipe of length $L \gg v_0 t$. An an exercise we show each step of the calculation in detail.

$$\begin{aligned}
\bar{P}(\mathbf{R}, t) &= \int_0^a dr \int_0^{2\pi} r\, d\theta \int_{-L/2}^{L/2} dz\, P(r, \theta, z)\, P(r, \theta, z | r + R, \theta + \Theta, z + Z, t) \\
&= \int_0^a dr \int_0^{2\pi} r\, d\theta \int_{-L/2}^{L/2} dz\, \frac{1}{\pi a^2 L}\, \delta(R)\, \delta(\Theta)\, \delta\left(Z - v_0\left(1 - {}^{r^2}/_{a^2}\right) t\right) \\
&= \int_0^a dr\, \frac{2r}{a^2}\, \delta\left(Z - v_0\left(1 - {}^{r^2}/_{a^2}\right) t\right)
\end{aligned} \tag{2.32}$$

Substituting the variable $\xi = v_0\left({}^{1-r^2}/_{a^2}\right) t$ we rewrite the integral

$$\begin{aligned}
\bar{P}(Z, t) &= \frac{1}{v_0 t} \int_0^{v_0 t} d\xi\, \delta(Z - \xi) \\
&= \frac{1}{v_0 t} H(Z - v_0 t)
\end{aligned} \tag{2.33}$$

where H is the hat function shown in Fig. 2.8. For laminar pipe flow, in the absence of diffusive effects, there is a uniform probability that the particles travel any distance between 0 and the maximum v_0t, or, in other words, an equal probability that the particle velocity lies between 0 and v_0, the peak velocity at the centre of the pipe.

2.2 Non-Newtonian fluids and viscoelasticity

Amongst the many applications of magnetic resonance insights regarding translational motion in fluids is that of rheological characterisation. Rheology concerns the study of various mechanical properties of non-Newtonian fluids, fluids for which a simple linear relation between stress and rate of strain does not hold. Indeed, the simple notion of liquids and solids is never exact, if we deform sufficiently rapidly or sufficiently slowly. For example, even water in the 'liquid' state may exhibit elastic properties if the rate of deformation is sufficiently high, while silicate glass may exhibit viscous flow if the

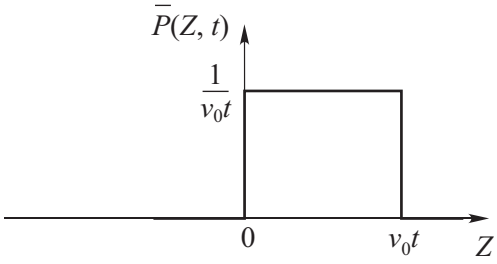

Fig. 2.8 Average propagator for axial displacements in Poiseuille flow.

observation time is sufficiently long. For all fluids the question of timescale is inherent, and in that sense all fluids are 'complex'. However, we generally assign the descriptors 'complex fluids' or 'complex soft matter' to those materials for which the timescales subdividing viscous and elastic behaviour are accessible in mechanical devices.

Complex fluids thus possess timescale complexity and both solid and liquid character. When these materials are subject to flow involving velocity gradients, their physical properties are generally non-linear, often anisotropic, and sometimes spatially heterogeneous. And all these properties have their origin in the molecular organisation and dynamics of each particular system. Hence, while the mechanical description of non-linear rheology is in itself an interesting and sometimes formidable area of engineering mathematics, the linking of these mechanical properties to underlying molecular organisation and dynamics represents one of the great challenges for modern chemical physics, a challenge that has resulted in beautiful new theories concerning the physics of polymers, colloids, and liquid crystals. And of course, this linkage has practical significance in modern materials science, in understanding the nature of biological tissue, the texture of food products, and the way in which fluids may be transported and processed. Rheology is a large field of research and one possessing a number of classic texts [16–25].

The use of magnetic resonance to study rheology is therefore doubly attractive. NMR has the potential to measure, *inter alia*, molecular orientation, intermolecular proximity, molecular re-orientational diffusion, and molecular translational Brownian motion. It is also capable of delivering an image of the local velocity field during the process of fluid deformation. In the case of NMR this information is provided non-invasively and without any requirement for optical transparency. Rheo-NMR is part the of the subject matter of Chapter 10.

2.2.1 Strain fields used in rheology

Effective rheological theories need to be able to handle any flow geometry that may be encountered in practise. However, for rheological characterisation there are a number of easily implemented geometries that allow the experimenter to gain access to relevant parameters of the constitutive behaviour. These generally involve simple cells in which one or more of the containment surfaces move. Figure 2.9 shows two implementations of shear fields using, respectively, cone-and-plate and cylindrical Couette cells,

approximating the idealised example shown in Fig. 2.4(a). Figure 2.10 approximates the idealised planar extension example of Fig. 2.4(b).

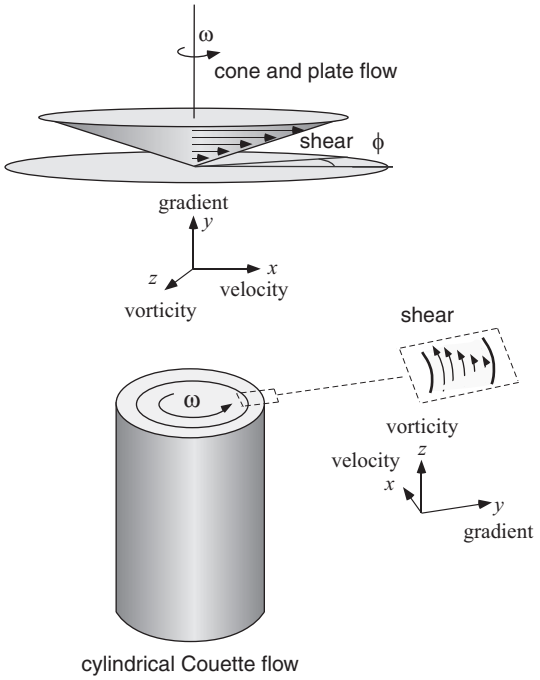

Fig. 2.9 Cone-plate and cylindrical Couette cells used to approximate a simple shear flow.

In simple shear, for which the velocity direction is taken to be x, one has $\kappa_{xy} = \dot{\gamma}$, all other $\kappa_{\alpha\beta}$ zero and

$$v_x = \dot{\gamma} y, \qquad v_y = 0, \qquad v_z = 0 \tag{2.34}$$

The coordinates (x, y, z) define the velocity, gradient, and vorticity axes, respectively.

In simple uniaxial elongational flow, with the axial extension direction taken as z, one has $\kappa_{zz} = \dot{\epsilon} = -2\kappa_{xx} = -2\kappa_{yy}$ and

$$v_x = -\frac{1}{2}\dot{\epsilon} x, \qquad v_y = -\frac{1}{2}\dot{\epsilon} y, \qquad v_z = \dot{\epsilon} z \tag{2.35}$$

This uniaxial extensional deformation can be achieved using a filament stretching rheometer.

By contrast, in planar axial flow, with the extension direction taken as z, $\kappa_{zz} = \dot{\epsilon} = -\kappa_{yy}$ and $\kappa_{xx} = 0$

$$v_x = 0, \qquad v_y = -\dot{\epsilon} y, \qquad v_z = \dot{\epsilon} z \tag{2.36}$$

In shear flow and extensional flow, the respective viscosities are defined by the ratios

$$\eta_S = \frac{\sigma_{xy}}{\dot{\gamma}} \tag{2.37}$$

and

$$\eta_E = \frac{(\sigma_{zz} - \sigma_{yy})}{\dot{\epsilon}} \tag{2.38}$$

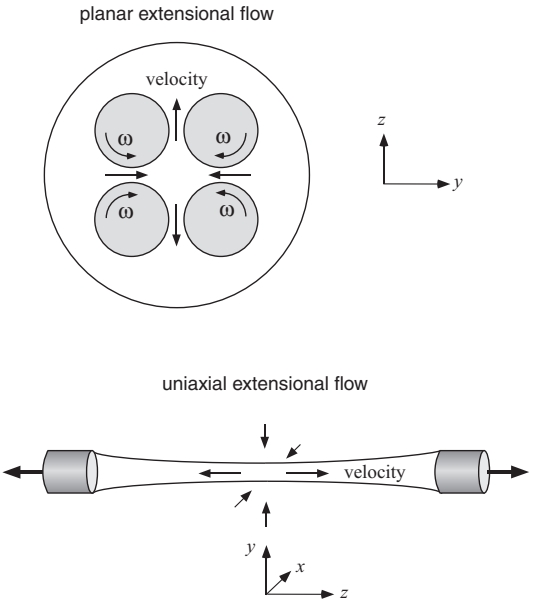

Fig. 2.10 Four roll mill [26] and filament stretch implementations [27] of planar and uniaxial extension, respectively.

The use of the difference of diagonal components of the stress tensor in the latter expression removes the effect of the isotropic term involving the pressure. Using eqn 2.15 it becomes clear that a Newtonian liquid has a uniaxial extensional viscosity $\eta_E = 3\eta_S$ (and planar extensional viscosity $4\eta_S$). The ratio of the extensional and shear viscosities is known as the Trouton ratio (T_r) and may greatly exceed 3 (in the planar case, 4) for viscoelastic fluids. Finally we note that unlike shearing flow, extensional flow cannot be experienced by an element of fluid in steady state in any practically realisable geometry. In consequence extension is always a transient phenomenon.

In the following sections we introduce some basic principles concerning the rheology of non-Newtonian viscoelastic fluids. Most of the discussion will concern shear deformation, although the ideas may be generalised to other deformations such as extensional flow.

2.2.2 Linear viscoelasticity

We start by considering a viscoelastic material deformed 'suddenly' by a small shear strain $\gamma \ll 1$, the strain being accompanied by a sudden stress, which gradually decays

as the molecules of the liquid rearrange themselves. Once the stress has decayed to zero the material has permanently deformed, and the elastic energy that was initially stored has dissipated, all 'memory' of the initial deformation being lost. Such a memory effect is characteristic of the material response of all viscoelastic fluids and the associated memory time (by comparison with the suddenness of the applied strain), will determine the extent to which our material can be regarded as solid or liquid.

For sufficiently small strains it is possible to treat the stress–strain response in a linear manner, and in practice the limits of such a linear description can always be found by measuring the extent of strain deformation over which the linear viscoleastic parameters are strain-independent. In the linear description [28] the stress response may be calculated by means of a memory function, $G(t)$, through the relation

$$\sigma(t) = \int_{-\infty}^{t} \dot{\gamma}(t')\, G(t-t')\; dt' \tag{2.39}$$

$G(t-t')$ gives the stress response of the system at time t when a rate of strain $\dot{\gamma}(t')$ is applied at an earlier time t'. It therefore represents the memory over the interval $(t-t')$. The characteristic time of the memory function, $G(t)$, is given by

$$\tau = \int_{0}^{\infty} \frac{G(t)}{G(0)}\, dt \tag{2.40}$$

Suppose at time $t' = 0$, a step shear strain γ is established at a rate that is very fast compared with τ ($ie\ \dot{\gamma} \gg \tau^{-1}$). Then $\dot{\gamma}(t')$ can be replaced by the Dirac delta function, $\gamma\,\delta(t')$ and eqn 2.39 reduces to

$$\sigma_{xy}(t) = \gamma\, G(t) \tag{2.41}$$

Hence we can see that the memory function is identified with the time-dependent shear relaxation modulus, which in turn may be measured directly from the step strain response.

If by contrast the shear strain γ is established at a rate that is very slow compared with τ, then $\dot{\gamma}$ is constant by comparison with $G(t-t')$ and, assuming that linearity holds, we obtain

$$\sigma_{xy}(t) = \dot{\gamma} \int_{-\infty}^{t} G(t-t')\; dt' = \dot{\gamma} \int_{0}^{\infty} G(t)\; dt \tag{2.42}$$

from which we can identify $\int_0^\infty G(t)\; dt$ as the Newtonian viscosity, η.

In general, the linear viscoelastic response of a material may be investigated by applying an oscillatory strain, $\gamma_0 \sin(\omega t)$, at small strain amplitudes ($\gamma_0 \ll 1$). Then the stress is given by

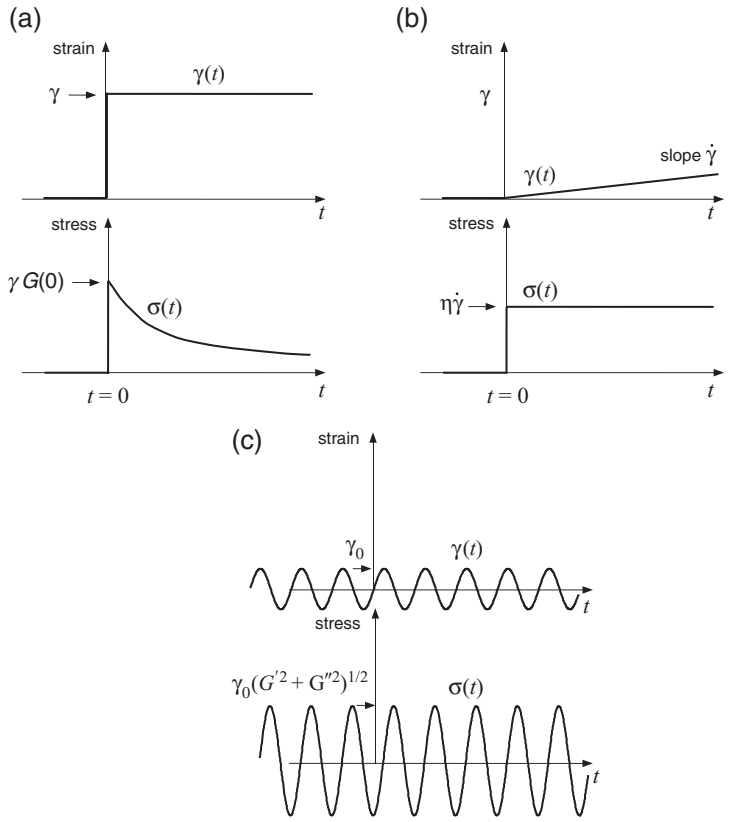

Fig. 2.11 Linear viscoelastic response of stress to (a) small step strain applied more rapidly than characteristic relaxation time τ, (b) steadily increasing strain applied at rate slow compared with τ, and (c) oscillatory strain. The phase shift between the stress and strain is a measure of the relative importance of the elastic and viscous responses.

$$\begin{aligned}
\sigma_{xy}(t) &= \int_{-\infty}^{t} \gamma_0\, \omega \cos(\omega t')\, G(t-t')\; dt' \\
&= \gamma_0\, \omega \int_0^{\infty} \cos(\omega(t-t''))\, G(t'')\; dt'' \\
&= \gamma_0 \left[\left\{ \omega \int_0^{\infty} \sin(\omega t'')\, G(t'')\; dt'' \right\} \sin(\omega t) \right. \\
&\qquad \left. + \left\{ \omega \int_0^{\infty} \cos(\omega t'')\, G(t'')\; dt'' \right\} \cos(\omega t) \right] \\
&= \gamma_0 \left[G' \sin(\omega t) + G'' \cos(\omega t) \right]
\end{aligned} \tag{2.43}$$

where G' and G'' are, respectively, the frequency-dependent storage and loss moduli and are directly related to the sine and cosine Fourier spectra of the memory function.

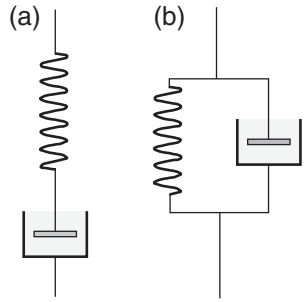

Fig. 2.12 (a) Maxwell and (b) Kelvin–Voigt spring dashpot representations of an 'elastic liquid' and a 'viscous solid', respectively.

Linear viscoelastic properties can be represented by suitable combinations of analogous dissipative and storage elements, such as dashpots and springs. One simple linear picture relevant to a viscoelastic liquid is the series dashpot-spring model of Maxwell shown in Fig. 2.12. The Maxwell memory function is exponential, namely, $G(t) = G_0 \exp(-t/\tau)$, with relaxation time $\tau_M = \eta/G_0$, where η is the viscosity of the dashpot fluid and G_0 is the elastic modulus of the spring. Similarly, viscous soft solids can be modelled using the Kelvin–Voigt model, in which the dashpot and spring are in parallel.

In general, one may model quite complex viscoelastic fluids whose characteristic dynamics cover a wide range of timescales by an appropriate superposition of Maxwell and Voigt elements [28], provided one is restricted to the range of strains for which the response is linear.

2.2.3 Non-linear viscoelasticity

Under sufficiently large strains, the mechanical response of all materials will differ from linear behaviour as a consequence of strain-induced structural rearrangements. For viscoelastic soft solids and liquids, the particular strain at which non-linear effects take over will depend on the details of the molecular structure, but will typically be on the order of unity. The subject of non-linear rheology is too extensive to be covered comprehensively here and readers are referred to a number of texts [17, 19, 22–25]. However, it is helpful to review one facet of non-linear rheology, namely the particularly common case of steady deformation, and to do so for one experimental geometry of interest, that of simple shear.

We start, in a quite general sense, by writing down the deformation over a finite time interval from t' to t as

$$\mathbf{r}(t) = \underline{\underline{\mathbf{E}}}(t, t') \cdot \mathbf{r}(t') \tag{2.44}$$

where the tensor $\underline{\underline{\mathbf{E}}}(t, t')$ describes the deformation history peculiar to the chosen strain geometry. Associated with $\underline{\underline{\mathbf{E}}}(t, t')$ will be a time- and strain-dependent stress in the fluid. Restricting ourselves to steady-state conditions, during which the rate of strain is held constant, results in a great deal of experimental and theoretical simplification. In this limiting case, non-linear viscoelastic behaviour is characterised by 'flow curves', the functions which describe the strain-rate dependencies of the stresses. The flow curve

shows the degree to which the structural rearrangements are able to compete with the external rate of deformation. Figure 2.13(a) shows a simple flow curve for a fluid that at low rates of strain behaves in a Newtonian manner, with constant viscosity, but for which the viscosity reduces above a certain characteristic strain rate $\dot{\gamma}_c$. That rate provides an indicator of the time scale, $\tau \sim {}^{1}/_{\dot{\gamma}_c}$, for structural rearrangement. The product $\dot{\gamma}_c \tau$ is commonly known as the Weissenberg number for steady shear deformation.

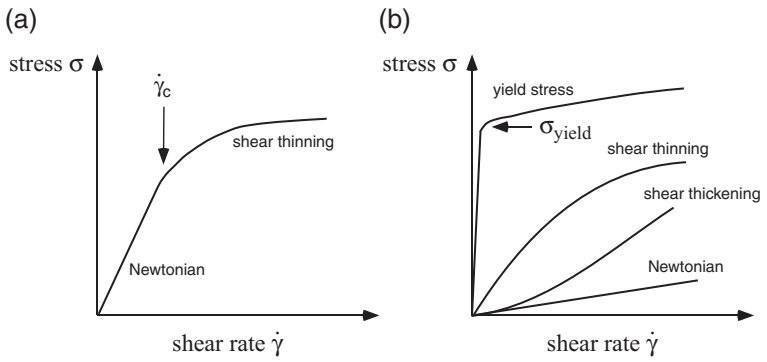

Fig. 2.13 (a) Transition from Newtonian to shear thinning behaviour at critical strain rate $\dot{\gamma}_c$ and (b) shear stress flow curves indicating a range of non-Newtonian behaviours in the non-linear viscosity.

For non-Newtonian viscoelastic liquids, non-linear flow may result not only in shear stress, but also in anisotropic normal stresses, describable by the first and second normal stress differences $(\sigma_{xx} - \sigma_{yy})$ and $(\sigma_{yy} - \sigma_{zz})$. In simple shear the constitutive relations for the fluid are given by

$$\sigma_{xy} = \eta(\dot{\gamma})\,\dot{\gamma}, \quad (\sigma_{xx} - \sigma_{yy}) = \Psi_1(\dot{\gamma})\,\dot{\gamma}^2, \quad (\sigma_{yy} - \sigma_{zz}) = \Psi_2(\dot{\gamma})\,\dot{\gamma}^2 \tag{2.45}$$

where $\eta(\dot{\gamma})$ is the shear-rate-dependent viscosity and $\Psi_1(\dot{\gamma})$ and $\Psi_2(\dot{\gamma})$ the first and second normal stress coefficients.

Figure 2.13(b) shows a family of shear stress flow curves in which a variety of non-Newtonian properties are exhibited, including yield stress, shear-thinning and shear thickening. A wide class of shear-thinning and shear-thickening fluids can be adequately described by a power law constitutive equation of the form

$$\sigma_{xy} = k\dot{\gamma}^n \tag{2.46}$$

for which $\eta(\dot{\gamma}) = k\dot{\gamma}^{n-1}$ and a Newtonian liquid has $n = 1$, while shear-thinning and shear-thickening liquids have $n < 1$ and $n > 1$, respectively. Of course such a description tells us nothing about the physical basis of non-linear viscosity.

In an equivalent sense, the rate-dependent non-linear extensional viscosity could be written as $\eta_E(\dot{\epsilon})$. However, since extension is always a transient phenomenon this viscosity must inevitably depend on time, t, or equivalently on the total (Hencky) strain $\epsilon = \int_0^t \dot{\epsilon}(t')\,dt'$, so that more correctly we should write the extensional viscosity as the function $\eta_E(\dot{\epsilon}, \epsilon)$.

2.3 Dispersion

Dispersion is the name we give to the phenomenon in which initially adjacent particles become separated during flow [15, 29]. The spreading and mixing that result from dispersion are of immense practical significance to a wide range of processes, such as oil recovery, ground water remediation, catalysis and the behaviour of packed bed reactors, filtration, chromatography, and biological perfusion. Dispersion is intrinsically governed by stochastic processes and, in this sense, has much in common with Brownian motion. However, whereas Brownian motion is driven by the stochastic fluctuations associated with molecular thermal energy, dispersion is driven by the subtle interplay of advective velocity gradients, molecular diffusion, and boundary layer effects, the latter being of particular importance in the flow of liquids or gases through a porous medium. While the language of dispersion has much in common with that used to describe self-diffusion, the range of phenomena available to be studied is, by comparison, considerably larger. Self-diffusion has unique characteristic lengths and timescales associated with molecular collisions, but in dispersive flow, multiple dynamical processes and structural features impart multiple length and timescales. Remarkably, many of those scales are accessible by NMR, either by magnetic resonance imaging methods or as ensemble averages over all streamlines, the latter obtained from the Lagrangian ensemble in which each molecule is labelled non-invasively by its local precession frequency. The details of how NMR accesses the various details of dispersive processes are left until later chapters. Here we review the essential physics of dispersion.

2.3.1 Stationary random flow and pseudo-diffusion

Before beginning a discussion of dispersion it is helpful to look at two simple examples of flow [30] that result in an isotropic, random distribution of molecular displacements. The first, which might be termed 'stationary random flow', has molecular motions randomly directed in magnitude and/or orientation and which are describable by an Eulerian velocity field, which is time-independent, and an ensemble of Lagrangian velocities, each of which is constant. This is the motion, illustrated in Fig. 2.14(a), which might be associated with laminar flow in an array of randomly directed capillaries in which the local director is fixed. The second, which we label 'pseudo-diffusion', involves molecular velocities that are not only randomly distributed across the ensemble but which fluctuate in time as well. Examples of pseudo-diffusion include turbulence and branched capillary motion, as shown in Fig. 2.14(b). Pseudo-diffusion is characterised by a correlation length l_c and correlation time τ_c.

The essential difference between these examples lies in the role of fluctuations, and in the time-dependence of mean-squared displacements. In stationary random flow, the absence of fluctuations leads to an inherent reversibility of the dispersion process, either by flow reversal or, as we shall see in the case of magnetic resonance tracer measurements, by reversing the sign of the flow-sensitive NMR parameter. The same reversibility is present in the dispersal caused by the Poiseuille velocity distribution for a single unidirected pipe (provided we neglect the effect of diffusion). Stationary random flow exhibits a quadratic dependence of mean-squared displacements on flow time. At times shorter than the flow time τ_c between branch points, the second flow geometry shown in Fig. 2.14(b) is indistinguishable from stationary random flow. But

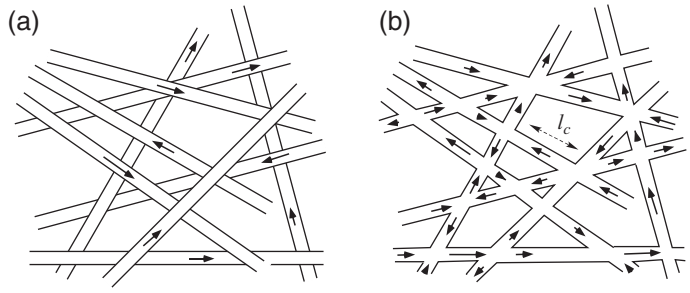

Fig. 2.14 (a) Stationary random flow and (b) pseudodiffusion.

at longer times, the mean-squared displacements become linear in time, akin to the Einstein relation for self-diffusion. This is the pseudo-diffusion regime. Whether the pseudo-diffusion dispersion process is reversible depends of course on the nature of streamline transitions at the branch points. Generally these transitions are at most only partially reversible. The reason for this has to do with the stochastic processes that underlie dispersion in heterogeneous flow fields.

2.3.2 Porous medium characteristics

Porosity and representative elementary volume

A porous medium can be regarded as the interpenetration of two regions in space, one from which fluid is excluded, and one which allows fluid ingress and flow: in the simplest of terms a solid matrix and an inter-connected pore space [31–33]. An illustration of such a medium is shown in Fig. 2.15. The measure that indicates the relative proportions of pore space and matrix is the porosity, ϕ, defined as the pore volume/total volume of medium. Of course it is possible that some pores may be entirely enclosed by the matrix, cut off from the interconnected pore space, but in what follows we shall be concerned only with those pores that contain fluid and therefore belong to the space that permits ingress.

An important characteristic of porous materials is the representative elementary volume (REV), defined as the smallest volume from which one can derive macroscopic properties. Bear [31] presents a nice way of visualising the REV, through the diagram shown in Fig. 2.16. Suppose one starts at some point inside the material and defines a volume ΔV_i surrounding that point. For example, the volume could be a sphere for which our point was the sphere centre. Now calculate a porosity ϕ_i, being the pore volume, ΔV_{pi} within ΔV_i, divided by the total volume ΔV_i. For large volumes the porosity is fairly constant but as the volumes are made smaller, the local porosity fluctuates, as shown in Fig. 2.16. In the limit, as $\Delta V_i \to 0$, ϕ_i will tend to 1 if the point chosen were in the pore space, or 0 if within the matrix. We may then define the REV as being the smallest volume, ΔV_0, beyond which the fluctuations are damped for further volume increases. This simple argument holds for a homogeneous porous medium. For a heterogeneous medium, there may exist longer length scales over which further changes in the mean porosity are observed, even though rapid variations with increasing ΔV_i, are no longer apparent.

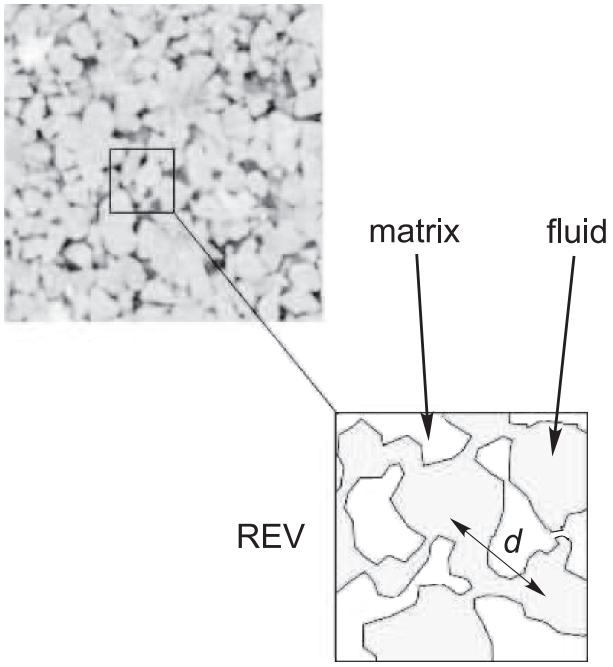

Fig. 2.15 Porous sandstone with schematic representative elementary volume (REV) indicated.

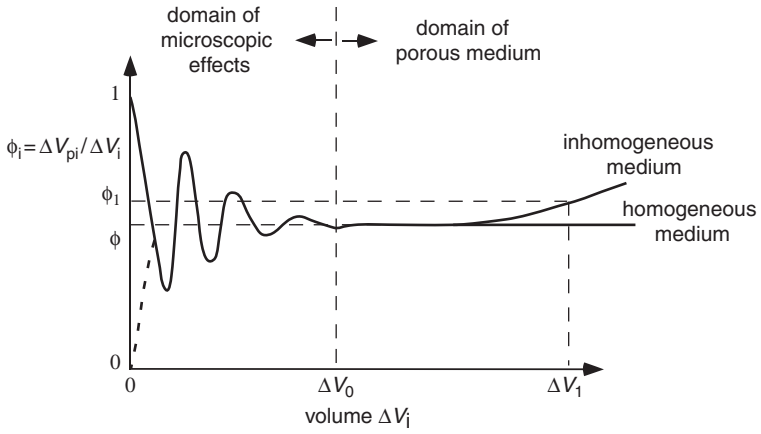

Fig. 2.16 Fluctuations in local porosity as the sampling volume is increased. For a homogeneous medium, there exists a volume ΔV_0, known as the representative elementary volume (REV) beyond which fluctuations are damped out. Heterogeneous materials may exhibit multiple volume and associated length scales. (Adapted from Bear [31].)

Permeability

The permeability, K_p, of the medium gives an indication of the ease with which fluid can be made to pass through the porous matrix, and its definition is due to Darcy in 1856 [34], in a relationship known as Darcy's law. For a fluid of dynamic viscosity η, the permeability is defined by the flow response to a pressure gradient dp/dz as

$$\langle v_z \rangle = -\frac{K_p}{\eta}\frac{dp}{dz} \tag{2.47}$$

where $\langle v_z \rangle$ is the average flow rate along the pressure gradient, as calculated from the volume flow rate across area A of $\dot{Q} = \langle v_z \rangle A$. In most descriptions of fluid flow in porous media, this mean flow rate, $\langle v_z \rangle$, derived from the volume rate, $\dot{Q}$, is known as the 'tube velocity', $\langle v_{\text{tube}} \rangle$. But of course, the fluid motion is confined to the interconnected pore space within the matrix, a space with a volume fraction ϕ. In consequence, an average tube velocity, $\langle v_{\text{tube}} \rangle$, translates to a larger average pore space velocity $\langle v \rangle$ by

$$\langle v \rangle = \frac{\langle v_{\text{tube}} \rangle}{\phi} \tag{2.48}$$

Characteristic lengths, characteristic times, and Péclet number

Inside the matrix the flow velocity fluctuates as molecules stream from pore to pore. The question then arises as to what size or volume is needed in order to calculate a faithful average of the flow. For this purpose we turn to REV, a volume larger than an average pore size (see Fig. 2.15). The length scale associated with the REV will be on the order of the longest correlation length of the pore space structure.

For fluid flow in a porous medium, a volume over which the Eulerian velocity field might be averaged suggests the existence of a suitable time over which the Lagrangian velocity might be averaged in order to obtain the same value of mean flow. Given the wide distribution of velocities present in porous media flow, it is reasonable to assume a wide distribution of correlation times, but there presumably exists a longest time beyond which a molecule has sampled all possible velocities in the Lagrangian ensemble and at which the dispersion may be said to be asymptotic.

A characteristic length shorter than the REV size is the mean pore size or, perhaps more appropriately, pore spacing d. [5] This length determines a fundamental correlation time defining the temporal structure of the velocity field, τ_v, the duration of flow around that characteristic length scale, and written

$$\tau_v = \frac{d}{\langle v \rangle} \tag{2.49}$$

Of course, a second fundamental time, essential to understanding the process of dispersion, is that required to migrate the pore distance by Brownian motion alone, namely $\tau_D \sim d^2/D$. The ratio of τ_D to the velocity correlation time, τ_v, provides a dimensionless number, the Péclet number, $Pe \sim d\langle v \rangle/D$, which characterises the flow dynamics.

[5] The question as to whether pore size or pore space spacing is the more relevant length is a moot point. We prefer to use the definition of pore spacing.

But what is the relevant value of D if we are describing the time to diffuse the mean distance, d, between pores? In defining τ_D, and hence the Péclet number, we need to settle on an appropriate length scale and diffusion coefficient. There are a number of different ways to define Pe for porous media. One convention [35] is

$$Pe = \frac{l\langle v\rangle}{D_0} = \frac{d\langle v_{\text{tube}}\rangle}{D_{\text{eff}}} \tag{2.50}$$

where D_0 is the unrestricted molecular diffusion coefficient. The characteristic dimension l is taken to be the effective pore spacing, defined by $l = \phi d/(1-\phi)$ and $D_{\text{eff}} = (1-\phi)D_0$ is an 'effective' or 'reduced' diffusion coefficient. Note that in this definition, Pe can also be regarded as the ratio of d^2/D_{eff}, 'the effective diffusion time to migrate the distance d' to $d/\langle v_{\text{tube}}\rangle$, 'the effective flow time to migrate a distance d'.

In the same way, it is possible to define the dimensionless Reynolds number that compares the magnitude of viscous and inertial forces to which the fluid is subjected, i.e.

$$Re = \frac{l\langle v\rangle}{\nu} = \frac{d\langle v_{\text{tube}}\rangle}{\nu_{\text{eff}}} \tag{2.51}$$

where ν_{eff}, by analogy to D_{eff}, is the effective kinematic viscosity.

The question then arises of what is the effective asymptotic ($t \gg \tau_D$) diffusion coefficient in the zero flow limit, $Pe = 0$, for molecules of a fluid imbibed in the pore space with self-diffusion coefficient, D_0. Clearly D_{eff}, as defined above, cannot suffice given its contrary dependence on porosity. Furthermore, porosity alone cannot determine the asymptotic diffusion since clearly pore connectivity plays a role. The generally accepted asymptotic result is

$$D^*\left(Pe = 0\right) = \frac{D_0}{\phi}\frac{\sigma}{\sigma_0} \tag{2.52}$$

where σ_0 is the electrical conductivity of the fluid and σ the electrical conductivity of the medium when occupied by the fluid. This result is mathematically derived in reference [36].

2.3.3 The dispersion tensor

In Chapter 1 the diffusion process was defined via the Fick's law diffusion equation (eqn 1.41) for the conditional probabilities, $P\left(\mathbf{r}|\mathbf{r}', t\right)$. In dispersion theory the same physics applies but with two significant changes. First, we must replace the time derivative by the substantive derivative, and second, we must allow that the dispersion will, in general, be anisotropic and hence represented by a tensor, $\underline{\underline{\mathbf{D}}}^*$, rather than the scalar diffusion coefficient, D. This anisotropy is an obvious consequence of symmetry-breaking by the flow. Hence

$$\frac{\partial}{\partial t}P\left(\mathbf{r}|\mathbf{r}', t\right) + \left(\mathbf{v}\cdot\nabla\right)P\left(\mathbf{r}|\mathbf{r}', t\right) = \nabla\cdot\left(\underline{\underline{D}}^*\,\nabla P\left(\mathbf{r}|\mathbf{r}', t\right)\right) \tag{2.53}$$

where $\mathbf{v}$ is the Eulerian velocity at $\mathbf{r}$. Solving eqn 2.53, in conjunction with the Navier–Stokes equation, for flow in the complex geometry of a porous matrix is a daunting

challenge. However, in the limit of long times, over which the dispersion may be said to be asymptotic, some considerable simplifications arise and indeed the nature of dispersion appears to follow a universal pattern.

The stochastic part of the flow

In the theory of dispersion, the roles of the Eulerian and Lagrangian perspectives are somewhat intertwined. While the Lagrangian approach provides some simplified definitions, when we seek information about spatial correlations a knowledge of the Eulerian velocity field is essential. For the moment, however, we will consider the ensemble of Lagrangian velocities $\{\mathbf{v}_L(t)\}$ [29, 37]. This distribution is characterised by an averaged velocity, $\mathbf{V}_L$, defined by $\mathbf{V}_L = \lim_{t\to\infty}\langle \mathbf{v}_L\rangle$, the ensemble average, $\langle \ldots \rangle$, being taken over the entire velocity distribution.

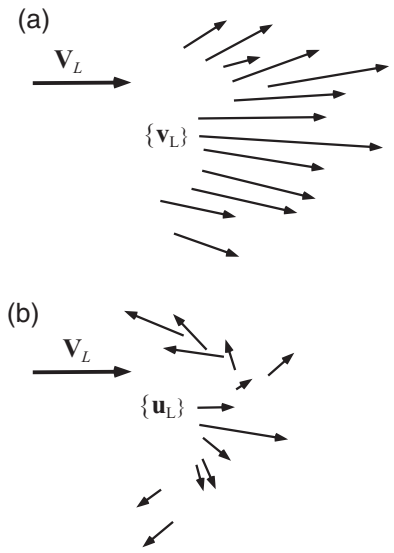

Fig. 2.17 (a) Ensemble of Lagrangian velocities $\{\mathbf{v}_L(t)\}$ with mean flow $\mathbf{V}_L$ and (b) same ensemble but for stochastic part $\{\mathbf{u}_L(t)\}$ (mean flow removed).

The fluctuation in the Lagrangian velocity may be defined by $\mathbf{u}_L(t) = \mathbf{v}_L(t) - \mathbf{V}_L$. It is the behaviour of $\mathbf{u}_L(t)$ and its distribution over the ensemble that contains the details of the dispersion process. For example, fluctuations in $\mathbf{u}_L(t)$ are described via the autocorrelation tensor, $\langle \mathbf{u}_L(\tau)\,\mathbf{u}_L(0)\rangle$, where the angled brackets refer to the ensemble average over the distribution of streamlines. We shall find the L subscript a nuisance in what follows and so, wherever u is a function of time only, we shall take it to be Lagrangian.

Clearly the averaged flow will be represented by a component of velocity, $V_\parallel$, parallel to the mean flow direction, the mean transverse component being zero. Equally, we may define stochastic components $u_\parallel$ and $u_\perp$. Since these will differ, we will expect

the nature of dispersion to be different when measured parallel or perpendicular to the mean flow.

Time-dependent and asymptotic dispersion tensor

Earlier we introduced the symbol $\mathbf{R}$ to define a displacement over some time t. Here we define the displacement $\mathbf{R}_u = \mathbf{R} - \langle \mathbf{R} \rangle$ that arises solely from the stochastic part of the velocity $\mathbf{u}$. We could represent $\mathbf{R}_u$ by the time integral of the velocity $\int_0^t \mathbf{u}(t')\, dt'$. Now consider the component of $\mathbf{u}$ parallel to the mean flow direction, denoting it $u_\parallel$. By direct analogy with the Einstein definition of diffusion[6] a longitudinal dispersion coefficient may be defined by [38]

$$D_\parallel^*(t) = \frac{1}{2}\frac{d\sigma_\parallel^2(t)}{dt} \tag{2.54}$$

where $\sigma_\parallel^2(t) = \langle \left(\int_0^t u_\parallel(t')\, dt' \right)^2 \rangle$.[7] Note that $D_\parallel^*(t)$ has an implied asymptotic limit

$$D_\parallel^* = \lim_{t\to\infty} \frac{1}{2}\frac{d\sigma_\parallel^2(t)}{dt} \tag{2.55}$$

Similarly we could define a transverse coefficient $D_\perp^*$.

The implication of anisotropy in the flow is that we will need to reconcile the Einstein description with the full tensorial representation of $\underline{\underline{D}}^*$. This is done by defining the dispersion tensor in a manner similar to that seen in Section 1.3.5. The dispersion tensor is given by [29, 38–40]

$$\underline{\underline{D}}^*(t) = sym \int_0^t \langle \mathbf{u}(\tau)\, \mathbf{u}(0) \rangle d\tau \tag{2.56}$$

with asymptotic limit

$$\underline{\underline{D}}^* = \lim_{t\to\infty} sym \int_0^t \langle \mathbf{u}(\tau)\, \mathbf{u}(0) \rangle d\tau \tag{2.57}$$

where $sym\left(\underline{\underline{A}}\right) = \frac{1}{2}\left(\underline{\underline{A}} + \underline{\underline{A}}^T\right)$. The tensorial nature of the dispersion is now apparent, since the ensemble average in the integrand of eqn 2.57 includes correlations between different velocity components. To understand how this definition relates to eqn 2.55, we note that the trace of this long timescale 'steady state' dispersion tensor yields a scalar dispersion coefficient that is simply related to the mean-squared displacements, $\sigma^2(t)$ via

$$\mathrm{Tr}\left(\underline{\underline{D}}^*\right) = \lim_{t\to\infty} \frac{1}{2}\frac{d\sigma^2(t)}{dt} \tag{2.58}$$

where $\sigma^2(t) = \langle \left(\int_0^t \mathbf{u}(t')\, dt' \right)^2 \rangle$.

[6]Note we here define a time-dependent diffusion coefficient in terms of a time derivative of mean-squared displacement, whereas the Einstein definition is strictly a mean-squared displacement divided by time. The significance of this difference in definition will be apparent in the discussion of asymptotic behaviour in Chapter 6.

[7]This is the fourth different use of the symbol σ after entropy, stress, and electrical conductivity. Context should provide a guide as to meaning.

The proof of eqn 2.58 is as follows. Consider two times, t_1 and t_2, such that $\tau = t_1 - t_2$. Then $\mathbf{R}_u(\tau) = \mathbf{R}_u(t_1) - \mathbf{R}_u(t_2)$ and

$$\mathbf{R}_u\mathbf{R}_u = \langle \mathbf{R}_u(t_1)^2 + \mathbf{R}_u(t_2)^2 - 2\,sym\,\mathbf{R}_u(t_1)\,\mathbf{R}_u(t_2)\rangle \tag{2.59}$$

Differentiation with respect to t_1 and t_2 gives

$$\frac{\partial^2 \mathbf{R}_u\mathbf{R}_u}{\partial t_1\,\partial t_2} = -2\,sym\,\langle \mathbf{u}(t_1)\,\mathbf{u}(t_2)\rangle \tag{2.60}$$

whence

$$\frac{\partial^2 \mathbf{R}_u\mathbf{R}_u}{\partial \tau^2} = 2\,sym\,\langle \mathbf{u}(t_1)\,\mathbf{u}(t_2)\rangle \tag{2.61}$$

We will assume that the ensemble is stationary, so that only the difference in time is relevant on the right-hand side of eqn 2.61. This means that $\langle \mathbf{u}(t_1)\,\mathbf{u}(t_2)\rangle$ may be replaced by $\langle \mathbf{u}(\tau)\,\mathbf{u}(0)\rangle$. Thus, on integrating, and noting $\sigma^2 = \mathrm{Tr}(\mathbf{R}_u\mathbf{R}_u)$, eqn 2.58 follows from eqn 2.57. Alternatively we may write

$$\underline{\underline{D}}^* = \lim_{t\to\infty} \frac{1}{2}\frac{d(\mathbf{R}_u\mathbf{R}_u)}{dt} \tag{2.62}$$

Dispersion mechanisms and scaling

The mechanisms that cause the flow-driven separation of initially adjacent molecules fall into three classes, known respectively as mechanical, diffusive, and holdup dispersion [35, 36, 39, 41]. Mechanical dispersion is due to stochastic variations in velocity induced by flow bifurcations in the advection of the fluid along tortuous paths. Diffusive (Taylor) dispersion [15] arises from molecular diffusion across streamlines. Holdup dispersion arises from boundary layer effects and from the presence of dead-end pores [39]. A simple illustration of these three processes is shown in Fig. 2.18.

The relative importance of these three mechanisms depends partly on flow geometry, but also on the value of Pe. Of course Taylor dispersion is always present, even in simple flows, whereas mechanical and holdup dispersion are a particular consequence of the complexity of flow associated with porous media. Remarkably, when non-dimensionalised against the molecular diffusion coefficient, D_0, and plotted against Péclet number, asymptotic dispersion in porous media follows a universal behaviour as shown in Fig. 2.19 for both ${}^{D^*_\parallel}/_{D_0}$ and ${}^{D^*_\perp}/_{D_0}$. Of course, when $Pe \ll 1$, the microscopic Brownian motion dominates and ${}^{D^*}/_{D_0} \sim 1$ (see eqn 2.52). For $Pe \gg 1$, D^* obeys an approximate power-law behaviour, ${}^{D^*_\parallel}/_{D_0} \sim Pe^\alpha$, where $1 < \alpha < 2$.

The non-dimensionalised mechanical dispersion might be expected to scale as Pe, since the rate of separation of molecules should depend linearly on both the velocity and the pore length scale. Similarly, we expect the non-dimensionalised asymptotic Taylor dispersion, arising from molecular diffusion across streamlines, to scale as Pe^2. The reason is as follows: in the asymptotic limit, the change in streamline velocity experienced by molecules as they sample all the pore space by diffusion transverse to the flow will be on the order of $\langle v\rangle$, while the time taken to traverse the flow by

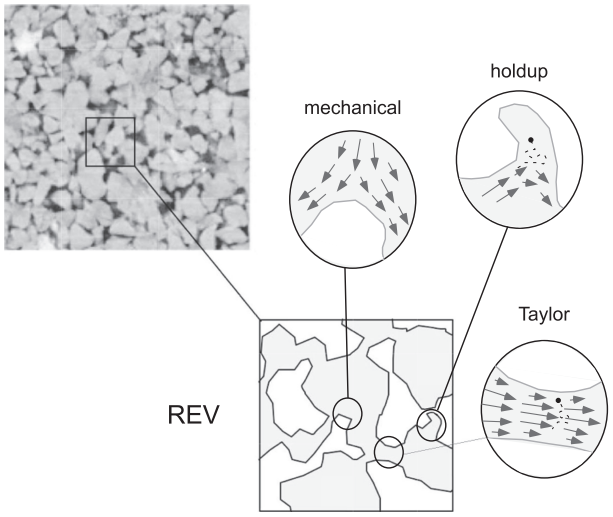

Fig. 2.18 Examples of mechanical, holdup, and Taylor dispersion.

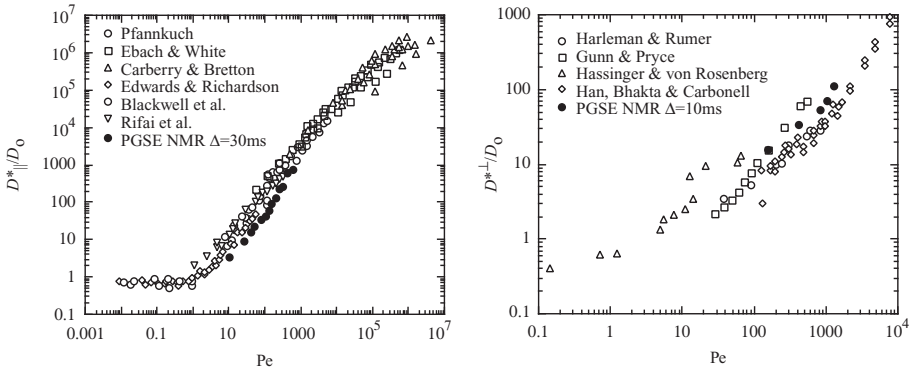

Fig. 2.19 Non-dimensional asymptotic dispersion coefficient vs Péclet number for dispersion longitudinal and transverse to the mean flow direction, taken from references [42, 43].

diffusion will be on the order of τ_D. Hence the mean-squared separation of molecules starting together will be $\langle v \rangle^2 \tau_D^2$, corresponding to a dispersion coefficient

$$\begin{aligned} D^*_{\text{Taylor}} &= \frac{\langle v \rangle^2 \tau_D^2}{\tau_D} \\ &= \frac{\langle v \rangle^2 l^2}{D_0} \end{aligned} \tag{2.63}$$

whence $D^*_{\text{Taylor}}/D_0 \sim Pe^2$. Holdup dispersion scales as $Pe \ln Pe$.

A simple example of porous medium dispersion is provided by flow through random bead packs, for which $\alpha \sim 1.2$, gradually reducing with increasing Pe. At the highest numbers for which measurements have been made, around 10^5 to 10^6, the asymptotic

longitudinal dispersion scales approximately as Pe, indicating the ultimate dominance of mechanical dispersion.

2.3.4 Taylor dispersion in pipe flow

As an illustration of Taylor dispersion in laminar flow, we here calculate the effect of diffusion across streamlines for Poiseuille flow in a cylindrical pipe of radius a. We will label the direction along the pipe axis z, and try to calculate the mean distance by which particles separate with respect to the mean flow. Of course even in the absence of diffusion perpendicular to the streamlines, shear alone will cause a particle separation. We will be able to identify that part of the dispersion in our result. And, we will always be able to add an additional longitudinal diffusion, D_0, which will be present in the absence of flow.

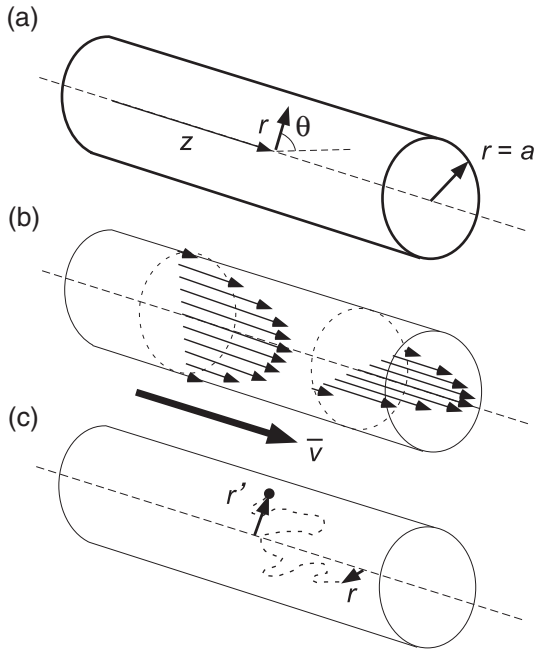

Fig. 2.20 Poiseuille flow in pipe showing (a) cylindrical polar coordinates, (b) velocity profile, and (c) diffusion across streamlines from starting radius r to final radius r'.

We start by writing down the axial displacement from origin at time t as $z\,(t)$. For Poiseuille flow, the mean axial flow rate, averaged across the pipe, is $\bar{v} = v_0/2$. Noting that $\langle z)t)\rangle = \bar{v}t$, the mean-squared axial displacement with respect to the mean flow is

$$\left\langle \left(z\,(t) - \bar{v}t\right)^2 \right\rangle = \left\langle z\,(t)^2 \right\rangle - \bar{v}^2 t^2 \tag{2.64}$$

while

$$\left\langle z\,(t)^2 \right\rangle = \int_0^t \int_0^t \left\langle v_z\,(\tau')\, v_z\,(\tau) \right\rangle d\tau d\tau' \tag{2.65}$$

$v_z(\tau)$ being the Lagrangian velocity at time τ. The problem then becomes one of tracking the history of particle velocities. The way we do this is to apply our knowledge of the steady-state Eulerian velocity field, $v_z(\mathbf{r})$, and to use a conditional probability $P(\mathbf{r}|\mathbf{r}', t)$ to determine how the particles move about in that field under diffusion [40]. Of course, given the velocity profile of eqn 2.23, it is clear that only radial displacements will change the velocity, and the problem in cylindrical polar coordinates reduces to a dependence on r only. Noting that the starting probability, $P(r, \tau)$ is independent of time and given by[8] $P(r) = 2/a^2$, we may write

$$\langle z(t)^2 \rangle = \int_0^t d\tau \int_0^t d\tau' \int_0^a r dr \int_0^a r' dr' P(r) P(r|r', \tau' - \tau) v_z(r) v_z(r') d\tau d\tau' \tag{2.66}$$

where[9]

$$P(r|r', \tau' - \tau) = \frac{2}{a^2}\left[1 + \sum_n \frac{J_0(\mu_n r/a) J_0(\mu_n r'/a)}{\mu_n^2 J_0(\mu_n)^2} \exp\left(-\frac{D_0 \mu_n^2}{a^2}(\tau' - \tau)\right)\right] \tag{2.67}$$

the J_0 being cylindrical Bessel functions with roots μ_n and D_0, the molecular self-diffusion coefficient. Note that eqn 2.67 is appropriate for $\tau' > \tau$ and that part of the integral $\int_0^t d\tau \int_\tau^t d\tau'$. To deal with the complementary case $\tau' < \tau$ we replace $P(r) P(r|r', \tau' - \tau)$ by $P(r) P(r'|r, \tau - \tau')$. The total integral $\int_0^t d\tau \int_0^t d\tau'$ is a sum of the identical complementary integrals and so

$$\begin{aligned}\langle z(t)^2 \rangle = &\left(\frac{2}{a^2}\right)^2 \int_0^t d\tau \int_0^t d\tau' \int_0^a r dr \int_0^a r' dr' v_z(r) v_z(r') \\ &+ 2\left(\frac{2}{a^2}\right)^2 \int_0^t d\tau \int_\tau^t d\tau' \int_0^a r dr \int_0^a r' dr' \Bigg[v_z(r) v_z(r') \\ &\times \sum_n \frac{J_0(\mu_n r/a) J_0(\mu_n r'/a)}{\mu_n^2 J_0(\mu_n)^2} \exp\left(-\frac{D_0 \mu_n^2}{a^2}(\tau' - \tau)\right)\Bigg]\end{aligned}$$

The first term in eqn 2.68 reduces to $\bar{v}^2 t^2$ and so the dispersive displacements with respect to the mean flow of eqn 2.64 become

$$\begin{aligned}\langle (z(t) - \bar{v}t)^2 \rangle &= 2 \int_0^t d\tau \int_\tau^t d\tau' \sum_n \frac{b_n^2}{\mu_n} \exp\left(-\frac{D_0 \mu_n^2}{a^2}(\tau' - \tau)\right) \\ &= 2\frac{a^2}{D_0} \sum_n \frac{b_n^2}{\mu_n^2} t - 2\left(\frac{a^2}{D_0}\right)^2 \sum_n \frac{b_n^2}{\mu_n^4}\left[1 - \exp\left(-\frac{D_0 \mu_n^2 t}{a^2}\right)\right]\end{aligned} \tag{2.68}$$

[8]Note that $P(r)$ has been averaged over azimuthal angle and is associated with rdr in the integrand.

[9]This result for the conditional probability associated with diffusion of molecules bounded by a cylindrical pipe is explained in Chapter 7.

where the b_n are radial integrals of the Bessel functions over the velocity distributions. Note the limiting cases

$$\lim_{t\to 0} \langle (z\,(t) - \bar{v}t)^2 \rangle = \sum_n b_n^2 t^2 \tag{2.69}$$

and

$$\lim_{t\to \infty} \langle (z\,(t) - \bar{v}t)^2 \rangle = 2\frac{a^2}{D_0} \sum_n \frac{b_n^2}{\mu_n^2} t \tag{2.70}$$

Of course, in the case of both equations, the independent axial diffusion contribution, $2D_0t$, should be added for a complete description.

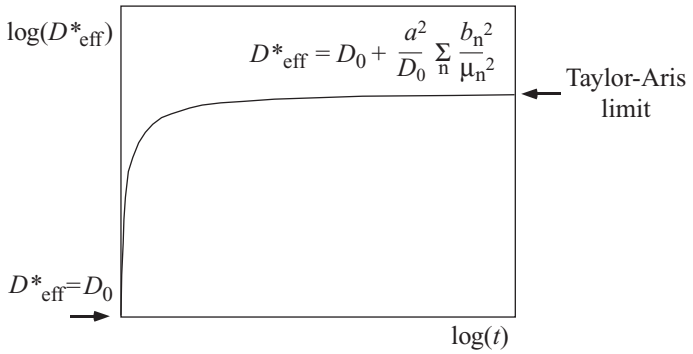

Fig. 2.21 Axial dispersion for flow in a pipe showing increase with time to Taylor–Aris limit.

The short time limit is dominated by the velocity shear across the pipe and contains no contribution from diffusion across streamlines. Accordingly, the quadratic time-dependence indicates that the mean-squared displacements are velocity-like rather than dispersion-like. Note that $\sum_n b_n^2 t^2 = {}^1\!/_3\, \bar{u}^2\, t^2$. As time increases, Taylor dispersion starts to play a role, reaching the limiting case when $t \gg {}^{a^2}\!/_{D_0}$. Equation 2.70 defines the Taylor–Aris asymptotic limit [44]

$$D^*_{\text{Taylor}} = D_0 + \frac{a^2}{D_0} \sum_n \frac{b_n^2}{\mu_n^2} \tag{2.71}$$

Figure 2.21 shows the gradual onset of the dispersive limit with increasing time. Intriguingly, as the molecular diffusion rate D_0 increases, the shear contribution to the asymptotic dispersion limit, D^*, decreases. This is an example of motional averaging at work. The faster the molecules diffuse to and fro between the bounding walls of the pipe, the less chance the velocity has to separate them down the flow axis as they cross the streamlines. Note again, given $b_n^2 \sim \bar{u}^2$, that ${}^{D^*_{\text{Taylor}}}\!/_{D_0}$ scales as Pe^2.

2.3.5 The velocity autocorrelation function and dispersion spectrum

The asymptotic dispersion tensor defined by eqn 2.57 can be viewed as the zero frequency component in the velocity autocorrelation function spectrum, which may be more generally defined by

$$\underline{\underline{D}}^{*}(\omega) = \frac{1}{2}\, sym \int_{-\infty}^{\infty} \langle \mathbf{u}(\tau)\, \mathbf{u}(0) \rangle \exp(i\omega\tau)\, d\tau \tag{2.72}$$

where we have taken advantage of the time reversal symmetry of $\langle \mathbf{u}(\tau)\, \mathbf{u}(0) \rangle$ to define the integral over all time.

The frequency-dependent dispersion tensor defined by eqn 2.72 has a spectral distribution dependent upon the characteristic correlation times for velocity fluctuations, τ_c. Let us for simplicity take a single component of velocity u_z. Noting eqns 1.27 and 1.28 and $\langle u_z \rangle = 0$, the mean correlation time is defined by the relation

$$\tau_c = \int_0^{\infty} \frac{\langle u_z(\tau)\, u_z(0) \rangle}{\langle u_z^2 \rangle}\, d\tau \tag{2.73}$$

From this definition we derive the zero-frequency amplitude of the dispersion tensor element D_{zz} as,

$$D_{zz} = \langle u_z^2 \rangle \tau_c \tag{2.74}$$

Finally, note that the definition of dispersion employed could allow for an ensemble in which the velocities, $\{\mathbf{u}\}$, do not vary with time but are simply a static distribution of zero mean. A good example is laminar flow in a straight pipe under conditions of minimal molecular self-diffusion. Such an ensemble will return a dispersion tensor that diverges with observation time, t. We will see that NMR gives us a means of distinguishing such behaviour from fluctuating flows.

2.3.6 Non-local dispersion

The dispersion tensor, as defined by eqn 2.56, has time-dependence, but is independent of spatial coordinates. In the language of fluid mechanics we say that the dispersion tensor is local, in the sense that it does not depend on the behaviour of the velocity field at other places. Indeed, by its very nature it is written in terms of Lagrangian velocities, which are not dependent on space. And, being formed by integrating the velocity autocorrelation function, is only weakly sensitive to its temporal structure, while in the asymptotic limit, $\underline{\underline{D}}^{*}$ is time-independent.

By comparison with the dispersion tensor, the covariant velocity autocorrelation function (VACF) is more fundamental in understanding fluid dispersion. In fact, we may dig deeper into the VACF and discover an even more fundamental correlation function, which depends not only on temporal displacement but also spatial displacement. Koch and Brady [37] have termed this the *non-local dispersion tensor*. It is the primary quantity describing details of the dispersion process. To understand the non-local dispersion tensor, one needs to link the Eulerian and Lagrangian descriptions. The key tool that enables this linkage is the conditional probability, the device that tells us the chance of finding a particle at two different places at two different times. The way we do this is illustrated in Fig. 2.22. Here, for clarity, we return to explicit use of L and E subscripts.

We will use this approach to rewrite the Lagrangian velocity autocorrelation function, i.e.

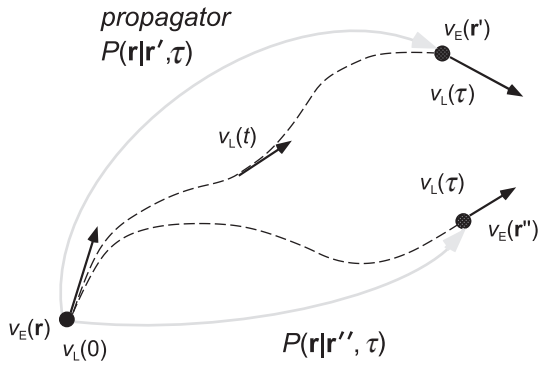

Fig. 2.22 The connection between the Eulerian velocity field and the ensemble of Lagrangian velocities at different times is given by the conditional probability $P(\mathbf{r}|\mathbf{r}',\tau)$.

$$\begin{aligned}\langle \mathbf{u}_L(\tau)\,\mathbf{u}_L(0)\rangle &= \iint P(\mathbf{r})\,\mathbf{u}_E(\mathbf{r},0)\;P(\mathbf{r}|\mathbf{r}',\tau)\,\mathbf{u}_E(\mathbf{r}',\tau)\;d\mathbf{r}\,d\mathbf{r}' \\ &= \iint P(\mathbf{r})\,\mathbf{u}_E(\mathbf{r},0)\;P(\mathbf{r}|\mathbf{r}+\mathbf{R},\tau)\,\mathbf{u}_E(\mathbf{r}+\mathbf{R},\tau)\;d\mathbf{r}\,d\mathbf{R}\end{aligned} \tag{2.75}$$

Equation 2.75 is obtained by writing a starting probability, $P(\mathbf{r})$, of being at position $\mathbf{r}$, and then using a conditional probability to find the subsequent chance to be at $\mathbf{r}'$ (or $\mathbf{r}+\mathbf{R}$), the full Lagrangian ensemble average being formed by integrating the Eulerian velocity product over all starting positions $\mathbf{r}$ and possible displacements $\mathbf{R}$. Note that for steady-state flow, the $\mathbf{u}_E(\mathbf{r},0)$ and $\mathbf{u}_E(\mathbf{r},\tau)$ in the above relations may be exchanged for their time-independent counterparts. The non-local dispersion tensor is then defined as the partial integrand

$$\underline{\underline{D}}^{NL}(\mathbf{R},\tau) = \int P(\mathbf{r})\,\mathbf{u}_E(\mathbf{r},0)\;P(\mathbf{r}|\mathbf{r}+\mathbf{R},\tau)\,\mathbf{u}_E(\mathbf{r}+\mathbf{R},\tau)\;d\mathbf{r} \tag{2.76}$$

This definition leads to the following integrals

$$\langle \mathbf{u}_L(\tau)\,\mathbf{u}_L(0)\rangle = \int \underline{\underline{D}}^{NL}(\mathbf{R},\tau)\;d\mathbf{R} \tag{2.77}$$

and

$$\underline{\underline{D}}^{*} = \iint \underline{\underline{D}}^{NL}(\mathbf{R},\tau)\;d\mathbf{R}\,d\tau \tag{2.78}$$

The hierarchy of integrations 2.77 and 2.78 provides special insight. Just as the spatial structure of $\underline{\underline{D}}^{NL}(\mathbf{r},\tau)$ is largely lost in the integration to form the velocity autocorrelation function, so in turn the VACF temporal structure is lost when further integration over time is required to obtain the local asymptotic dispersion tensor. Given that perspective, one may regard the non-local dispersion tensor as a primary quantity that retains maximum information. Of course $\underline{\underline{D}}^{NL}(\mathbf{R},\tau)$ is not strictly a dispersion tensor in a dimensional sense. Rather, it is a full spatio-temporal correlation function, nine elements in the symmetric velocity correlation tensor, three dimensions in spatial offset $\mathbf{R}$, and one more dimension in the time offset, τ, sufficiently rich in information that its measurement represents a worthy challenge.

References

[1] Judges 5:4,5.

[2] R. E. Meyer. *Introduction to Mathematical Fluid Dynamics*. Dover, New York, 1982.

[3] D. J. Acheson. *Elementary Fluid Dynamics*. Oxford University Press, Oxford, 1990.

[4] T. E. Faber. *Fluid Dynamics for Physicists*. Cambridge University Press, Cambridge, 1995.

[5] R. A. Granger. *Fluid Mechanics*. Dover, New York, 1995.

[6] F. M. White. *Fluid Mechanics*. McGraw-Hill, New York, 2003.

[7] G. K. Batchelor. *An Introduction to Fluid Dynamics*. Cambridge University Press, Cambridge, 1967.

[8] L. D. Landau and E. M. Lifschitz. *Fluid Mechanics 2nd Edition*. Butterworth-Heinemann, Boston, 1987.

[9] O. Reynolds. An experimental investigation of the circumstances which determine whether the motion of water shall be direct or sinuous, and of the law of resistance in parallel channels. *Philosophical Transactions of the Royal Society*, 174:935, 1883.

[10] J. L. M. Poiseuille. Physiques - recherches experimetales sur le mouvement des liquides dans les tubes de tres petits diametres. *Academie des Sciences, Comptes Rendus*, 111:961 and 1041, 1840.

[11] S. Succi. *The Lattice Boltzmann Equation for Fluid Dynamics and Beyond*. Oxford, New York, 2001.

[12] P. L. Bhatnagar, E. P. Gross, and M. Krook. A model for collision processes in gases. I. Small amplitude processes in charged and neutral one-component systems. *Phys. Rev.*, 94:511, 1954.

[13] D. Wolf-Gladrow. *Automata and Lattice Boltzmann Models*. Springer, New York, 2001.

[14] M. C. Sukop and D. T. Thorne. *Lattice Boltzmann Modeling: An Introduction for Geoscientists and Engineers*. Academic Press, New York, 2007.

[15] G. I. Taylor. Dispersion of soluble matter in solvent flowing slowly through a tube. *Proc. Roy. Soc. A*, 219:186, 1953.

[16] A. S. Lodge. *Elastic Liquids*. Academic Press, New York, 1964.

[17] A. S. Lodge. *Body Tensor Fields in Continuum Mechanics*. Academic Press, New York, 1974.

[18] K. Walters. *Rheometry*. Chapman and Hall, London, 1975.

[19] R. B. Bird, R. C. Armstrong, and O. Hassager. *Dynamics of Polymeric Liquids*. Wiley, New York, 1977.

[20] J. D. Ferry. *Viscoelastic Properties of Polymers*. Wiley, New York, 1980.

[21] R. I. Tanner. *Engineering Rheology*. Oxford, New York, 1985.

[22] M. Doi and S. F. Edwards. *The Theory of Polymer Dynamics*. Oxford, London, 1986.

[23] R. G. Larson. *Constitutive Equations for Polymer Melts and Solutions*. Butterworths, Boston, 1987.

[24] H. A. Barnes, J. J. Hutton, and K. Walters. *An Introduction to Rheology*. Elsevier Amsterdam, 1989.
[25] R.G. Larson. *The Structure and Rheology of Complex Fluids*. Oxford, New York, 1998.
[26] G. I. Taylor. The formation of emulsions in definable fields of flow. *Proc. Roy. Soc. A*, 146:501, 1934.
[27] G. H. McKinley and T. Sridhar. Filament-stretching rheometry of complex fluids. *Annual Review of Fluid Mechanics*, 34:375, 2002.
[28] N. W. Tschoegl. *The Theory of Linear Viscoelastic Behaviour*. Springer, New York, 1980.
[29] J. F. Brady. Dispersion in heterogeneous media. In E. Guyon J. P. Hulin, A. M. Cazabat and F. Carmonas, editors, *Hydrodynamics of Dispersed Media*. Elsevier, New York, 1990.
[30] P. T. Callaghan. *Principles of Nuclear Magnetic Resonance Microscopy*. Oxford University Press, New York, 1991.
[31] J. Bear. *Dynamics of Fluids in Porous Media*. Elsevier, New York, 1972.
[32] F. A. Dullien. *Porous Media*. Academic Press, New York, 1992.
[33] W. Ehlers and J. Bluhm (eds). *Porous Media: Theory, Experiments and Numerical Applications*. Springer, New York, 2002.
[34] H. Dary. *Les Fontaines Publiques de la Ville de Dijon*. Dalmont, Paris, 1856.
[35] M. Quintard and S. Whitaker. Transport in ordered and disordered porous-media – volume-averaged equations, closure problems, and comparison with experiment. *Chem. Eng. Sci.*, 48:2537, 1993.
[36] J. Koplik, S. Redner, and D. Wilkinson. Transport and dispersion in random networks with percolation disorder. *Phys. Rev. A*, 37:2619, 1988.
[37] D. L. Koch and J. F. Brady. A nonlocal description of advection diffusion with application to dispersion in porous-media. *J. Fluid Mech.*, 180:387, 1987.
[38] H. Brenner. Dispersion resulting from flow through spatially periodic porous-media. *Phil. Trans. Roy. Soc. London A*, 297:81, 1980.
[39] J. Salles, J. F. Thovert, R. Delannay, L. Prevors, J. L. Auriault, and P. M. Adler. Taylor dispersion in porous-media – determination of the dispersion tensor. *Phys. Fluids*, 5:2348, 1993.
[40] C. Van Den Broeck. Taylor diffusion revisited. *Physica A*, 168:677, 1990.
[41] O. A. Plumb and S. Whitaker. *Dynamics of Fluids in Hierarchical Porous Media*, chapter Diffusion, Adsorption and Dispersion in Porous Media: Small Scale Averaging and Local Volume Averaging. J. H. Cushman, ed., Academic Press, San Diego, 1990.
[42] J. D. Seymour and P. T. Callaghan. Generalized approach to NMR analysis of flow and dispersion in porous media. *AIChE J.*, 43:2096, 1997.
[43] A. A. Khrapitchev and P. T. Callaghan. Reversible and irreversible dispersion in a porous medium. *Physics of Fluids*, 15:2649, 2003.
[44] R. Aris. On the dispersion of a solute in a fluid flowing through a tube. *Proc. Roy. Soc.*, A 235:67, 1956.